Influence of the performance of triple and double glazing on the fire development in a dwelling

Huizinga, R.A.

Award date:
2012

Influence of the performance of triple and double glazing on the fire development in a dwelling

Master thesis

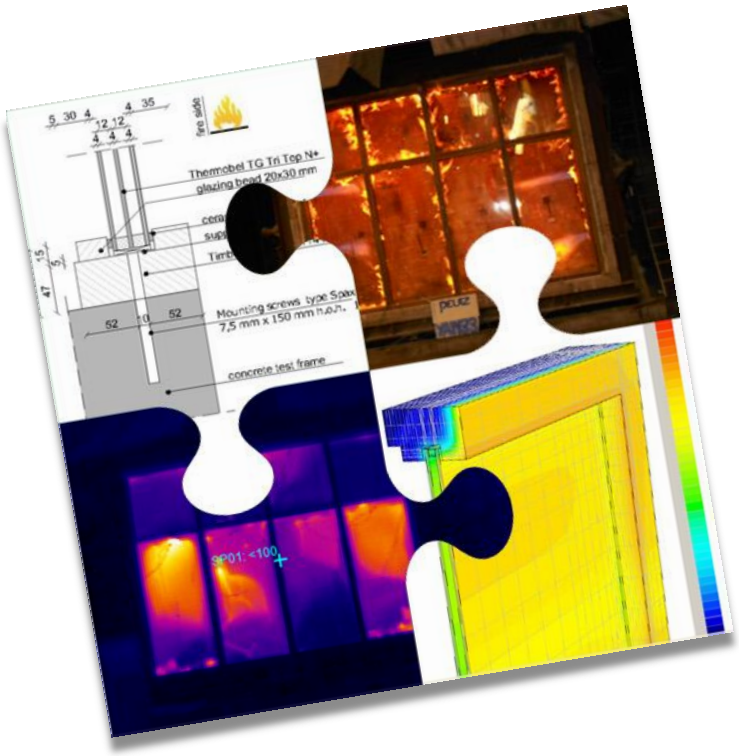

Author: R.A. Huizinga

Supervisors: Prof. ir. W. Zeiler (1st faculty supervisor TU/e)
Dr. ir. M.G.L.C. Loomans (2nd faculty supervisor TU/e)
Ir. R. van Herpen (fellow TU/e)

Department: Building Physics & Services
Department of Architecture, Building and Planning
Eindhoven University of Technology

Date: 4 December 2012

Version: Final (version 1)

Acknowledgement

This thesis is the end product of my graduation project at the Eindhoven University of Technology of the department Building Physics and Services. I am very grateful for the pleasant cooperation with the involved companies, to mention: Peutz, Timmerfabriek de Mors Rijssen, AGC Flat glass Nederland, and Nieman Raadgevende Ingenieurs. Without the support of these participants this graduation thesis would not have been possible. I want to thank Gerard Winkel, Jacques Mertens, and Joris van der Vleuten for the pleasant cooperation, and shared knowledge during the preparation of the experiment. Also I would like to thank my supervisors Marcel Loomans, Wim Zeiler and Ruud van Herpen for their guidance, insight and shared knowledge. Furthermore, I would like to thank Stefan van de Wetering, Niek van Dijk, and Menno Huizinga for their practical insights and help during the assembly. Finally I would like to thank my family and girlfriend for their support throughout this project.

Peutz B.V.
Montageweg 5
6045 JA Roermond

Timmerfabriek de Mors Rijssen B.V.
Nijverheidsstraat 41
7461 AD Rijssen

AGC Flat Glass Nederland B.V.
Panovenweg 21
4004 JE Tiel

Nieman Raadgevende Ingenieurs
Dokter van Lookeren Campagneweg 16
8004 DC Zwolle

Abstract

The application of double glazing is wide spread in the current house stock, energy efficient dwellings will lead to the application of triple glazing. Glass fallout is an important factor that influences the fire development during an enclosure fire. A smouldering fire seems more likely when the glazing system remains intact, while a flaming fire will be more likely in a situation with major glass fallout. A smouldering fire will in general lead to a higher toxicity hazards for the occupants or the right conditions for a backdraft. A flaming fire, on the other hand can lead to flash-over conditions. Therefore it is imperative to know which fire scenario will be more likely, in order to anticipate on it with adequate measures. Until today assumptions are made about the performance of triple glazing in relation to glass fallout during fire without any scientific basis. This Master thesis is initiated to obtain an insight on the time before glass fallout of triple and double glazing systems during an enclosure fire in a dwelling. The following research question is brought up to approach the subject: ‘*’To what extend does the fallout period of triple glass affect the indoor fire conditions in dwellings differently compared to the fallout period of double glazing?’*’ The graduation thesis is based on experimental research with the use of a fire furnace and supporting simulations to assess the likelihood of a fire scenario in a dwelling. The two presented experiments consist of a double and triple glazing assembly with four large and four small windows. Individual temperatures of the glass surface, shaded area, and temperature differences were analysed in relation to glass fallout. The analysis of the results revealed a wide spreading between temperatures and glass fallout. Engineering correlations, such as the internal energy in gasvolume and the maximum temperature before glass fallout were established to quantify the difference in performance between triple and double glazing. The results show a detectable difference between the performance, and provide an indicative criterion of glass fallout as a result of internal energy in gasvolume. Additionally a comparison is made between the experimental results and reference literature on the performance of double glass to verify the found criterion in relation to a vertical temperature gradient.

A calibration of the simulation model is performed in order to retrieve some specific conditions during the experiment with the fire furnace. The results enable an assessment of the representativeness of the fire experiment to a typical enclosure fire. The assessment indicated that the conditions during the experiment might result in a less pronounced radiation level than one would expect during an enclosure fire. Because the difference is not consistent for each temperature, it is difficult to quantify the difference in radiation.

Subsequently various fire scenarios were defined to obtain an indication of the probability of glass fallout during an enclosure fire. The assessment of various fire situations is related to the experimental found criterion and takes into account various boundary conditions such as difference in construction, geometry, type of fire, and ventilation inlets. These results have led to new insights on the probability of an altered fire scenario for dwellings with multi-pane glazing.

One must keep in mind that the given estimation is bound by several limitations. At first only one specific temperature curve is used, which allows only the assessment of the fire scenarios which remain under the given maximum limits. Furthermore, the results only apply for the same compositions and glazing assemblies. Also the experimental study consists of a small sample size, making a statistical approach unreliable. These limitations, combined with the different conditions of the fire furnace compared to an enclosure fire, emphasises a certain nuance on the found conclusions.

Table of Contents

Terminology

Traditional dwelling	A dwelling which complies with the minimum requirements according the Dutch building code 2003 is referred in this study as a regular/standard dwelling. This also implies that a potential fire will most likely behave as a fuel controlled fire.
Energy efficient dwelling	An energy efficient dwelling is in this study referred to as a dwelling which is equipped with an improved thermal envelope compared to a traditional dwelling, (which in turn may influence the fire behaviour). These technical measures consist of a higher thermal envelope in combination with triple glazing and higher leakage proofing. (This also implies that a potential fire might behave as a ventilation controlled fire).
Passive house	A passive house is a sustainable dwelling that uses minimal energy consumption for heating and cooling which is respectively lower than 15 kWh m^2, and with total energy consumption lower than 42 kWh m^2. In order to achieve these low energy consumptions the passive house must have an envelope with a high thermal resistance and a sustainable installation.
Smothered or smouldering fire	In this study a smothered fire will be related to fire without actual flames due to a minimal supply of oxygen. This fire will in turn cause more smoke development and has a higher toxicity. Furthermore a smouldering fire will be ventilation controlled.
Flaming fire	A flaming fire is generally fuel controlled and will have the potential to reach to a flashover situation, provided there is enough fuel. Generally a flaming fire will produce more heat and less smoke then a smouldering fire
Toxicity	Toxicity is measured as the dose of a gas that will lead to death or incapacitation (often known as untenable conditions). Toxicity of gases is expressed in parts per million (ppm).
OFP	Overall Failure Probability (OFP) expresses the probability of an initial crack in a glass pane during a fire.
HRR	The Heat Release Rate (HRR).
Half width	The half width defines the dimensions of a window.
Shading thickness	The shading thickness defines the length of the shielded area of the glass along the edge due to the groove in the window frame.
Absorption	Logarithmic ratio between the radiation upon a material and transmittance through a material.
CFD	Computational Fluid Dynamics (CFD) stands for a simulation tool.
FDS	Fire dynamics simulator simulation software (based on CFD)
SDOM	Spectral discrete ordinates radiation model (SDOM) simulation tool
Temperature difference	The temperature difference refers in this study to the difference in temperature between the central glass surface and the shaded temperature.

Nomenclature

Symbol	Property	unity
S	Surface	m^2
V	Volume	m^3
$\dot{V}$	Flow rate	m^3/s
Q	Quantity of heat	J
Q_{rad}	Quantity of heat through radiation	W
Q_{conv}	Quantity of heat through convection	W
P	Power / capacity	W
q	Density of heat flow rate	W/m^2
I	Radiation intensity	W/m^3
I_t	Radiation intensity passed through a material	W/m^3
T	Temperature	$^oC/K$
λ	Thermal conductivity	W/mK
u	U-value	W/m^2K
σ	Constant of Stefan-Boltzmann ($5.67 \cdot 10^{-8}$)	W/m^2K^4
ε	Emissivity of a material	-
$\lambda_{\mu m}$	Wavelength	μm
α	Thermal diffusivity	m^2/s
C_p	Specific heat capacity at constant pressure	J/kgK
ρ	Density	kg/m^3
β	Linear coefficient of expansion	$1/^oC$
E	Tensile/elastic modulus (Young's modulus)	GPa
σ_b	Breaking stress	MPa
d*	Penetration depth	M
μ	Poisson-constant	-
h_c	Convective heat transfer coefficient	W/mK
q_i	Incident radiation density	-
a_{qi}	Absorption factor	-
r_{qi}	Reflection factor	-
t_{qi}	Transmission factor	-
p	Pressure	Pa
ppm	Parts per million	ppm
ΔT	Temperature difference in glass	^oC
TΔ	Difference compared to initial temperature	^oC
B	Factor for a specific product	-
θ_s	Surface temperature	K
θ_∞	Temperature of the liquid or gas	K
t	Time	S
h_c	Convective heat transfer coefficient	W/m^2K
E_g	Internal energy in gasvolume	KJ/m^3
K	Boltzmann constant ($1.38066 \cdot 10^{-23}$)	J/K
S_p	Smoke potential	$m^{-1}m^3/kg$
S_d	Smoke density	m^{-1}
$\dot{Z}$	Massflow of solid smoke particles	m^2/s
Z	Mass of solid smoke particles	m^2
H_c	Heat of combustion	J/kg
R	Individual gasconstant (286.9)	J/kg K

1 Introduction

According to the Dutch CBS (Central Buro of Statistics), approximately half of all deathly casualties during an enclosure fire occur in residential buildings, making fire safety in dwellings an important topic. The risk of casualties depends on various characteristics such as the building occupants, the present fire load, and the building envelope. The last two characteristics determine the indoor conditions during a fire, which can be translated to tenability limits for the occupants. The building envelope is adapting on the demand for sustainability from traditional constructions to envelopes with high insulation and air tight facades. Recent studies by Cornil et al. (2010) and Molkens (2011) have indicated that an enclosure fire in an energy efficient dwelling or a passive house behaves differently compared to a traditional dwelling due to the new building methods. These studies suggest a kind of smouldering fire for energy efficient dwellings, which in turn might cause specific toxicity hazards for the occupants or the right conditions for a backdraft. Figure 1 gives an schematic overview of fire scenario's which can be expected during a ventilation controlled fire. A traditional dwelling, on the other hand, is expected to face a fuel controlled fire, which can lead to a flashover situation. Figure 2 gives an schematic overview of fire scenario's which can be expected during a fuel controlled fire.

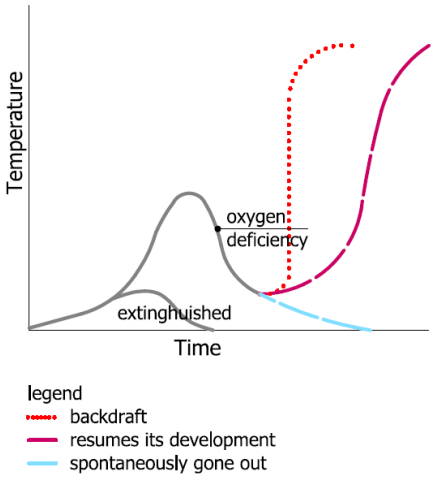

Figure 1: ventilation controlled fire scenarios

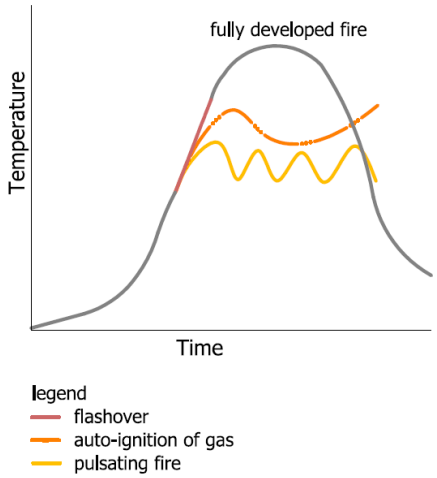

Figure 2: fuel controlled fire scenarios

From the characteristics of the building envelope, the ventilation inlets in the form of open or closed windows c.q. doors will be the most decisive factor for the fire scenario in small enclosures, which are typical for dwellings. This study provides more insight on the time before multi-pane glazing will function as an oxygen inlet (fallout) during a fire. The results will enable a better prediction of the fire scenario in a dwelling. The implementation of these insights combined with adequate advice and fire safety measures will hopefully improve the fire safety in dwellings.

1.1 Problem statement

Both the study by Cornil et al (2011), and the study by Molkens (2011) are based on the assumption that glazing in a traditional dwelling will fallout at an early stage in a fire, while triple glass in an energy efficient dwelling will remain intact. However, this assumption is not supported by any scientific basis. Until today no comprehensive studies exist, within the current knowledge of the author, which addresses the performance of triple glazing during fire. Therefore, this study is initiated to give more insight on this subject and to check if the assumption involving glass fallout is justified.

1.2 Research objective

There can be distinguished two objectives which will be pursued:

- obtaining an insight of the critical boundary conditions before the occurrence of glass fallout for triple glazing compared to double glazing with the use of a fire furnace;
- stocktaking of the probability on glass fallout in relation to various fire situations in an enclosure.

These combined objectives will provide an estimation of the probability on a different fire scenario in a traditional dwelling compared to an energy efficient dwelling as a consequence of the performance of the glazing.

1.3 Research question

The following research question is posed to approach the subject concerning the problem statement:

''*To what extend does the fallout period of triple glass affect the indoor fire conditions in dwellings differently compared to the fallout period of double glazing?*''

Different sub questions are defined in order to answer the research question:

- What is the difference in performance of triple glazing compared to double glazing in relation to glass fallout?
- Is the experimental rig with a fire furnace representative for an enclosure fire in a dwelling?
- Which fire scenarios might lead to glass breakage for double and triple glazing?

1.4 Researchmodel and approach

Figure 3 gives the research method which is maintained during this study. The orientation phase consists of an introduction and a description of the theory for glass breakage caused by fire conditions. The primary subject of this study consist of an experimental research to assess the performance of triple and double glazing with the use of a fire furnace. The method will discuss the boundary conditions and measurement setup. The results will compare the performance between triple and double glass in relation to glass fallout. The second part will involve simulations to support the experimental research. Finally the experimental results are compared to results from simulated enclosure fires in dwellings. The discussion will link both main subjects and will describe the remaining limitations and uncertainties. This will eventually lead to conclusions and recommendations on the influence of triple and double glass on the fire scenario.

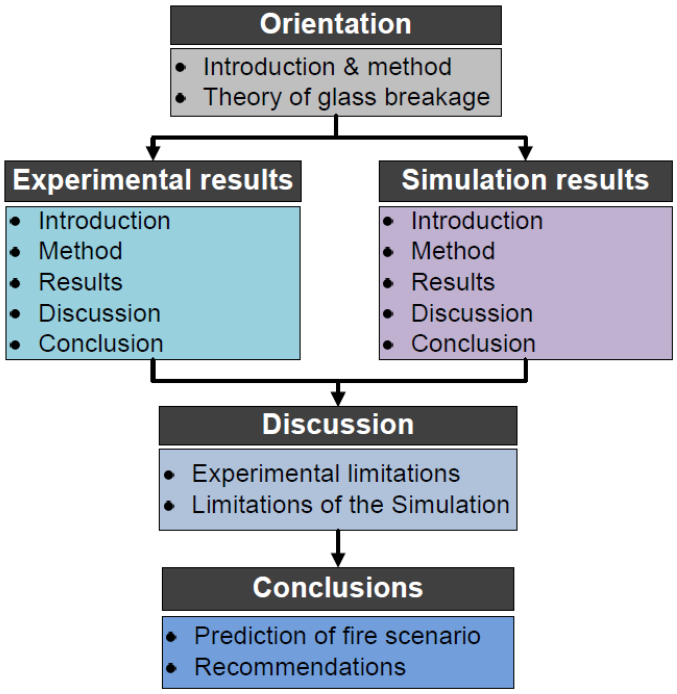

Figure 3: research model

1.5 Theoretical basis

In order to comprehend the presented study it is appropriate to provide some theory about glass breakage and the used physics. The following sections will discuss this theory.

1.5.1 Breaking mechanism of glass

The thermal breaking mechanism of glass can be categorized in the following categories (Keski-Rahkonen, 1988, p. 3):

- *Intensive heat flux*: if an intense heat flux is suddenly applied on one side of a glass pane, a steep thermal gradient will be created across the thickness of the layer. This phenomena is called ''thermal shock'' and causes thermal stresses which could break the pane;
- *Thermal gradient*: a thermal gradient over the thickness of the pane will cause the planar plane to deform. The boundary conditions (edge conditions, glass type etc.) will cause stresses which are the largest in the corners of the plane. These stresses could become particular high in very small panes, controversially for the larger panes which are more flexible;
- *Non-uniform heating*: thermal stresses and tension will occur when the glass pane is not uniformly heated. This situation occurs when parts of the glass are shaded from radiation, which is the case for the shielded edge of the window by the shading of the frame. As a result the maximum stress will always occur at the rim of the pane. The non-uniform heating between the central glass pane and the shaded area will be addressed in this study as the temperature difference (ΔT).

Besides the higher stresses along the edges of the pane, the area can also contain micro cracks due to the cutting process. These manufacturing imperfections can also contribute to cracks and eventual early fallout of the entire window. The non-uniform heating is in practice the most normative parameter during a fire. Additionally pressure variations could also potentially affect the failure of glass planes. However, the influence of pressure will be beyond the scope of the present study.

1.5.2 Underlying physics

For a thorough analysis of the experimental results it is appropriate to split the convective and radiant heat transfer mechanism, because they have a different principle of heat transfer to the glass. When the temperature rises the radiation part of heat will increase with the power of four (see equation 1), making radiation the most dominant heat mechanism during an enclosure fire. Additionally, the soot particles in the hot gas layer will radiate heat directly on the surface. The radiation from the fire itself can also have a contributing factor, dependable on the location of the fire source to a surface. The heat share due to convection (equation 2) will take a sub-ordinary role when the temperature increases to high levels. The heat transfer mechanism during the experiment with the fire furnace, on the other hand, will consist for a large part of convection. Radiation occurs only as a result of the direct flames from the gas burners and of the refractory bricks inside the fire furnace.

$$Q_{conv} = h \cdot A \cdot (\theta_s - \theta_\infty) \quad [W] \quad (1)$$

with:
Q = convective heat [W]
h_c = convective heat transfer coefficient [-]
A = surface [m^2]
θ = temperature [^oC]

$$Q_{rad} = \sigma \cdot {\theta_s}^4 \quad [W] \quad (2)$$

with
Q = radiant heat [W]
σ = Constant of Stephan-Boltzmann [W/m^2K^4]
θ = temperature [^oC]

The amount of energy that is needed in order to raise a substance to a predetermined temperature level is defined by equation 3. This equation will be used as means to calculate the amount of energy which is used for the temperature rise in the fire furnace.

$$Q = \rho \cdot C_p \cdot T\Delta \qquad [\mathrm{J/m^3}] \qquad (3)$$

with:
Q = quantity of heat [W]
ρ = density [kg/m^3]
C_p = specific heat capacity [J/kgK]
TΔ = difference compared to initial temperature [^{o}C]

Subsequently, through the use of the ideal gas law, the change in density of the gasvolume as consequence of the temperature rise can be derived by the use of equation 4. Conditions for the use of this method are a constant pressure, and a constant volume, which is a reasonable assumption during this experiment. Although the fluctuation in pressure during the experiment was marginal, it is included in the calculation for the completeness.

$$\rho_{gas_2} = \frac{p}{R \cdot T_1} \qquad [\mathrm{kg}] \qquad (4)$$

with:
p = pressure [Pa]
T = temperature [K]

The internal energy inside the fire furnace can be derived by calculating the integral of the energy over time, which is compensated by the expansion in gasvolume. Equation 5 provides a method to compare the internal energy in gasvolume in the fire furnace, to an internal energy in gasvolume obtained through the natural fire concept for a reference building.

$$\frac{\int_0^{t_3} Q_{g^2}}{t_{total}} = \frac{\int_0^{t_4} E_{g^3}}{t_{total}} \qquad [\mathrm{KJ/m^3}] \qquad (5)$$

E_g = internal energy in gasvolume [KJ/m^3]
t = time [s]

Convective heat will be transformed to radiation and conduction when in contact with the glass. This transformation can be expressed in the convection coefficient. The radiation density is dependent on the properties of the heated material, angle of incidence, and the radiation spectrum. During an enclosure fire the most radiant energy will occur in the infrared spectrum between the 0.4 μm and the 4.0 μm respectively. Figure 4 illustrates the relative intensity of a typical flame for free burning gasoline. A typical ideal radiant surface, or black body, has an emission factor of 1. Glass, on the other hand, is almost 100% transparent in the visible spectrum for radiation, while it is opaque in the infrared spectrum for the wavelengths which are of interest during a fire. The presence of the coating will enhance the reflective properties. The optical properties of soda lime silica glass are well defined for the solar spectrum under stable temperature conditions by Rubin, 1985. These properties for higher temperatures are scarce, since they are investigated in few studies as also confirmed by personal communication by Dr. ir. Dembele 13-10-2012, and Dr. ir. Abdelghany 9-10-2012. Figure 5 illustrates the spectral absorption coefficient of Soda Lime Silica glass as a function of temperature derived by Gardon (1958) on a logarithmic scale. The stationary energy properties of glass according to AGC (2012) such as the transmission and reflection can be found in appendix III. The thermal properties of other materials which are used in the assembly are in general well defined. The thermal conductivity of Argon gas under various pressures and temperatures is established in

[1] Conditions over time in the fire furnace
[2] Internal energy in gasvolume inside the fire furnace
[3] Internal energy in gasvolume according to the natural fire curve

the study by Tiesinga et al, 1994. The viscosity and thermal conductivity of dry air under various conditions are provided by the study of Kadoya et al, 1985. The studies by Zeller & Pohl (1971), Ades et al (1990), and Khalil et al (2009) established the thermal conductivity and specific heat for Soda Lime Silica glass under increasing temperature conditions.

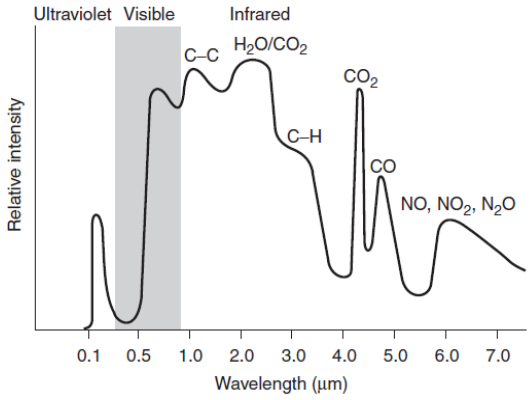

Figure 4: Spectrum of a typical flame (free burning gasoline) NFPA handbook (2008)

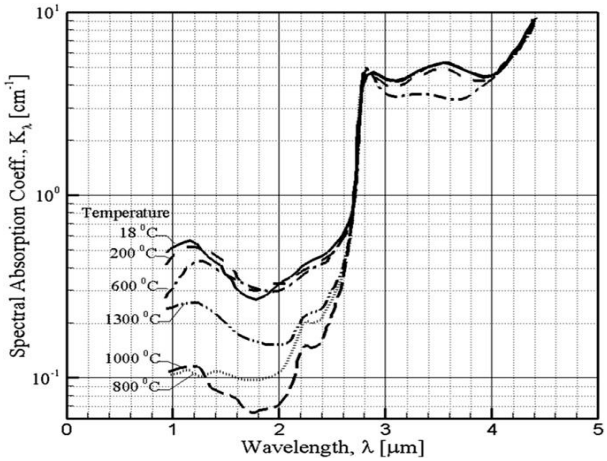

Figure 5: Spectral absorption coefficient of SLS glass Gardon (1958)

Equation 6 gives the incident radiation density for transparent materials such as glass in relation to the absorption, reflection and transmission.

$$q_i = a + r + t \tag{6}$$

with:
q_i = incident radiation density [-]
a = absorption factor [-]
r = reflection factor [-]
t = transmission factor [-]

The absorption of glass is defined by equation 7, where the intensity of radiation is divided by the intensity that is passed through a material.

$$a_{\lambda_{\mu m}} = \log_{10}\left(\frac{I}{I_t}\right) \tag{7}$$

with:
I = radiation intensity
I_t = radiation intensity passed through a material
$\lambda_{\mu m}$ = wavelength [μm]

The radiation temperature for two infinite parallel planes can be derived through equation 8 where emitted[4] temperatures by a surface are radiated to a receiving[5] surface.

$$q_r = \varepsilon_{res}\sigma(T_5^4 - T_6^4) \tag{8}$$

with:
ε = emissivity of a material

[4] Temperature of the radiant surface
[5] Temperature of the receiving surface

The radiation temperature is based on a black body as defined by equation 9. The combined emission of two materials, as described in equation 11, can be derived through equation 10.

$$q_r = \varepsilon \sigma T^4 \qquad (9)$$

$$\varepsilon_{res} = \frac{1}{\frac{1}{\varepsilon_5} + \frac{1}{\varepsilon_6} - 1} \qquad (10)$$

The lumped heat capacity model provides a simplified method to determine the heating of glass. This method neglects the influence of direct radiation by the fire source and takes only into account the heating through the hot gas layer. The lumped heat capacity model is defined by equation 10.

$$\rho \delta C_p \frac{dT_g}{dt} + h_{hot} \cdot \left(T_g - T_0\right) = q''(t) \qquad (11)$$

The lumped capacitance model divides a thermal system in a number of discrete lumps with the assumption that the difference inside each lump is negligible. Both the glass panes as the inner cavity will function as a poor heat conductor, causing temperature gradients over the thickness of the layers. However, the glass pane itself is relatively thin (four mm in this case), therefore the model can provide a working approximation for the heating of a solid. The temperature before the occurrence of the initial crack can be defined by equation 12, which is based on the temperature difference between the central glass and the shaded temperature as given by equation 13.

$$\sigma_b = \frac{E \cdot \beta \cdot \Delta T}{1 - \mu} \cdot B \quad [\text{GPa}] \qquad (12)$$

$$\Delta T > \frac{\sigma_b \cdot (1 - \mu)}{E \cdot \beta} \cdot B \quad [^{o}\text{C}] \qquad (13)$$

with:
E = elastic modulus [GPa]
β = Linear coefficient of expansion [1/°C]
μ = Poisson-constant [-]
B = factor for a specific material [-]

with
Q = radiant heat [W]
σ = Constant of Stephan-Boltzmann [W/m^2K^4]
θ = temperature [°C]

Solving the equation for 4 mm float glass, for a single glazing construction, gives a maximum temperature difference of 61.91 °C, before the occurrence of initial crack in the glass pane. The glass properties which are maintained as input can be found in appendix III. However, this global calculation can only give a conservative lower limit for the occurrence of cracks and is therefore inadequate to give a prediction of glass fallout. A slightly more accurate approach can be achieved through the integration over the thickness of the pane as given by equation 14.

$$\Delta T = \frac{g \sigma_b}{E \beta} = \left(\frac{1}{L}\right) \int_0^L T(x,t) dx - T_i \qquad (14)$$

The finite element method as provided by Dembele et al (2012) gives a comprehensive method to assess glass breakage in relation to the first crack. This method is based on spectral discrete ordinates radiation models. Therefore it takes into account the spectral sensitivity of the glass in the infrared spectrum. In addition it takes mechanical stresses into account. Deviations due to different boundary conditions are approached through a statistical Weibull distribution. This method seems promising in near future applications to calculate the moment of glass fallout. However, due to the increasing complexity and deviations which are involved with glass fallout, it is still necessary to expand this method towards this specific application. The glazing systems with one or two cavities increase the complexity even further, making it impossible to use this method at this time.

2 Fire furnace Experiment with double and triple glazing

2.1 Introduction

Results of two fire experiments in which a double and triple glazing assembly were exposed to a fire furnace are presented and discussed. The dimensions of the fire furnace are according to the ISO 834 standard, with respectively 3.0 m in height, 4.05 m in width, and 0.75 m in depth. The goal will be to obtain an indication about the time before the occurrence of glass fallout.

2.2 Experimental rig

The experimental rig and maintained method during the experiment is discussed in Appendix I. The experimental rig, as discussed in this paragraph, will provide a summary of the boundary conditions and used method. The measurement setup consist of four small windows at the upper section of the frame and four large windows at the lower level, with dimension of respectively 924 by 924 mm (0.854 m^2) and 1897 x 924 mm (1.753m^2). The sample frame with double glazing consists of 6 windows with standard double glass and 2 windows of HE++ (high-efficiency) glass. The sample frame with triple glazing consists entirely of the same type of triple glass (8 windows). The composition of the frame is identical for both glazing assemblies. The seam along the concrete test frame is sealed with Rockwool insulation. Figure 6 gives an overview of the dimensions and numbering of the glazing assembly.

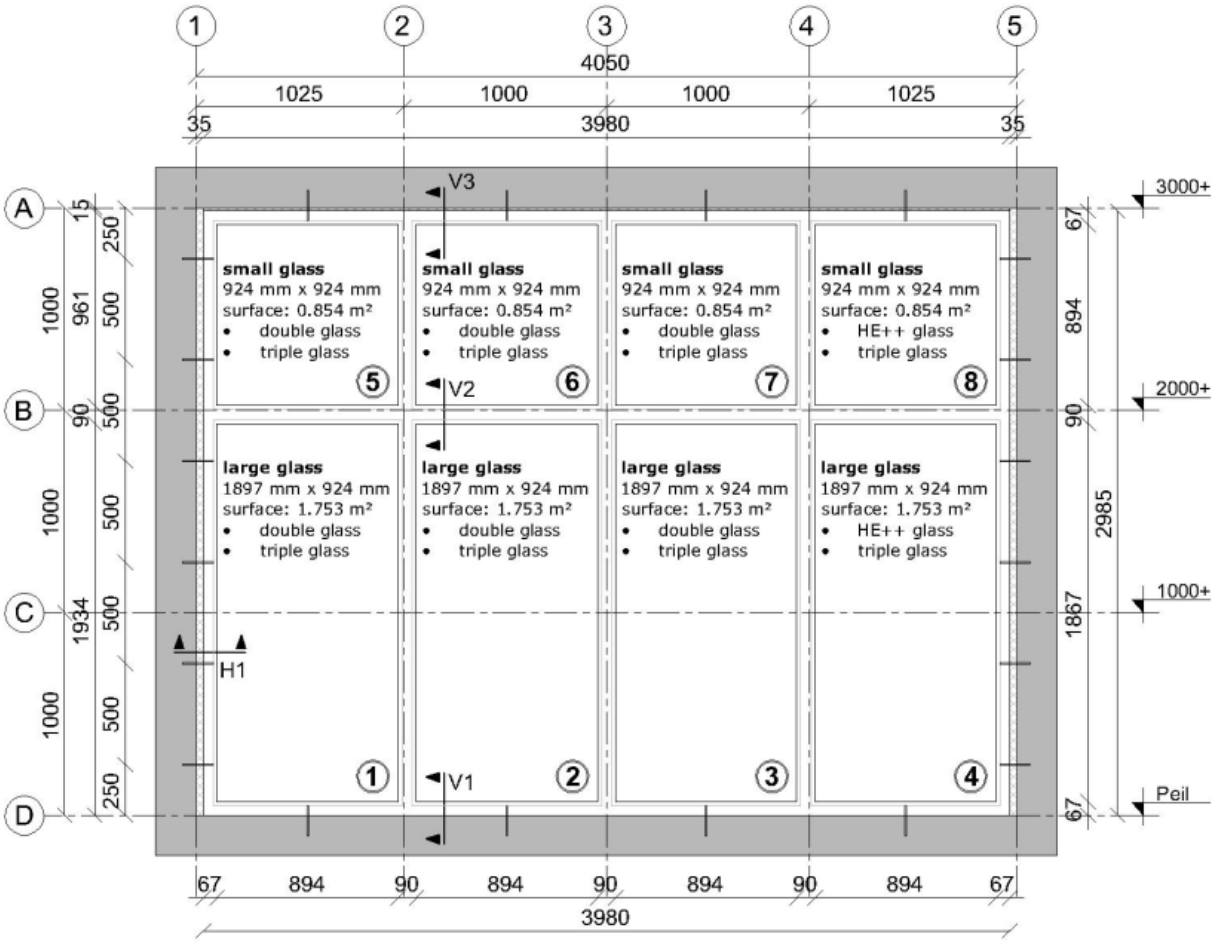

Figure 6: experimental assembly

The standard double glazing consists of a composition with two panes of 4 mm Soda Lime Silica glass and a cavity in-between of 12 mm filled with 90% Argon gas. The composition of the triple

glass is approximately similar, and consists of two cavities of 12 mm filled with 90% Argon gas and three panes of 4 mm Soda Lime Silica glass. Both HE++ and triple glazing are equipped with a coating on the inner side of the inner pane, additionally triple glass has a coating on the inside of the outer pane. Standard double glazing is not equipped with a coating. The dimensions of the windows are more or less the same as maintained in the full-scale fire experiments of double glazing by Shields, Silcock, and Flood (1998), and Shields et al (2005). Also the thicknesses of the pane and the cavity have the same dimensions. This approach will enable a comparison, to some extent, between the results of this experiment and the mentioned reference study. The timber frame is constructed from a solid piece of Mahogany without rotating parts. The posts in the frame are 20 mm high. The shading thickness of the glass is 15 mm in length, leaving a gap of 5 mm around the glass and the timber frame. The gaps on the lateral sides of the glass are 4 mm in width and are filled with a ceramic bracelet. Figure 7 gives the composition in detail for the triple and double glazing samples. The composition of the detail is in accordance to the standard processing instructions of AGC (2012).

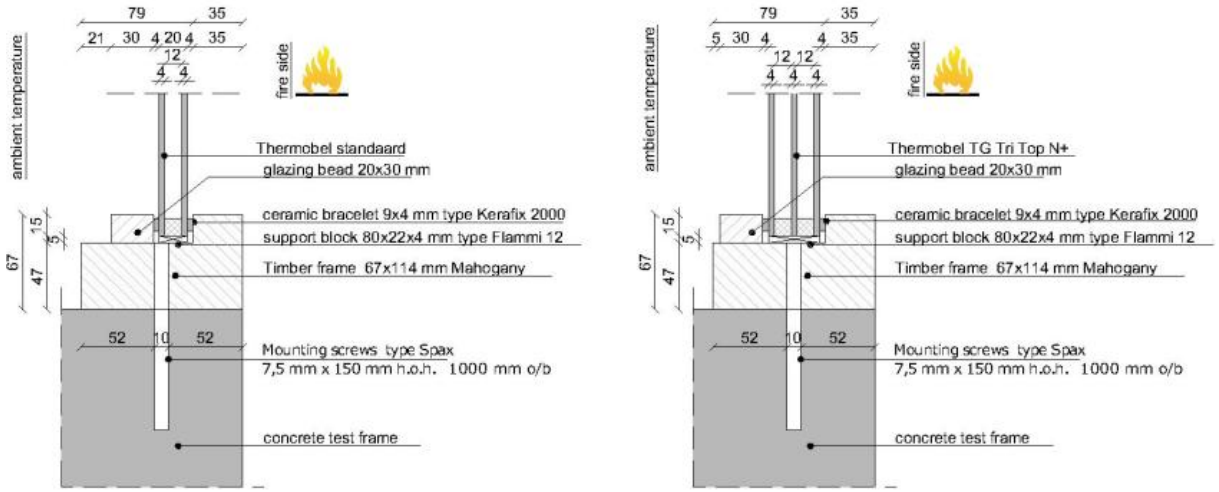

Figure 7: detail of the timber frame

Table 1 describes the specific composition and insulation properties of the maintained glazing systems. The Soda Lime Silica (SLS) float glass consists approximately of 75% SIO_2, 15% NA_2O, and 10% CaO%.

Name	Type	Composition [mm]	U-value [W/(m²·K)]
Double glass	Thermobel standard	4 - 12 Ar 90% - 4	2.7
HE++	Thermobel Top N+	4 – 12 Ar 90% - 4	1.3
Triple glass	Thermobel TG Tri Top N+	4 – 12 Ar 90% - 4 – 12 Ar 90% - 4	0.7

Table 1: glazing systems

The temperature inside the fire furnace can be raised according to various fire curves. These fire curves are in daily practise used for classifying the fire resistance of construction-elements, and are unrelated to the temperature development in case of an enclosure fire. The standard fire curve according to NEN-EN 1363-1 is based on flashover-conditions, to replicate a fully developed fire scenario. This scenario would be expected after glass fallout in an enclosure. In case of a ventilation controlled fire the temperatures will be much lower. Additionally it is more evident to assess the performance of multi-pane glazing during the initial phase of the fire. The slow heating curve according to NEN-EN 1363-2, seems to be more suitable to resemble the initial phase of an enclosure fire. The influence of thermal shock will be less prominent due to the more gradual temperature rise, which one would also expect during an enclosure fire. The slow heating curve will increase in severity after 21 minutes. This will enable also an assessment of the performance during higher temperatures, which might also be the case for

some situations. For these reasons, the slow heating curve gives the most suitable temperature development, and provides at the same time a reproducible method. Figure 8 gives the graph of the slow heating curve in relation to the standard fire curve.

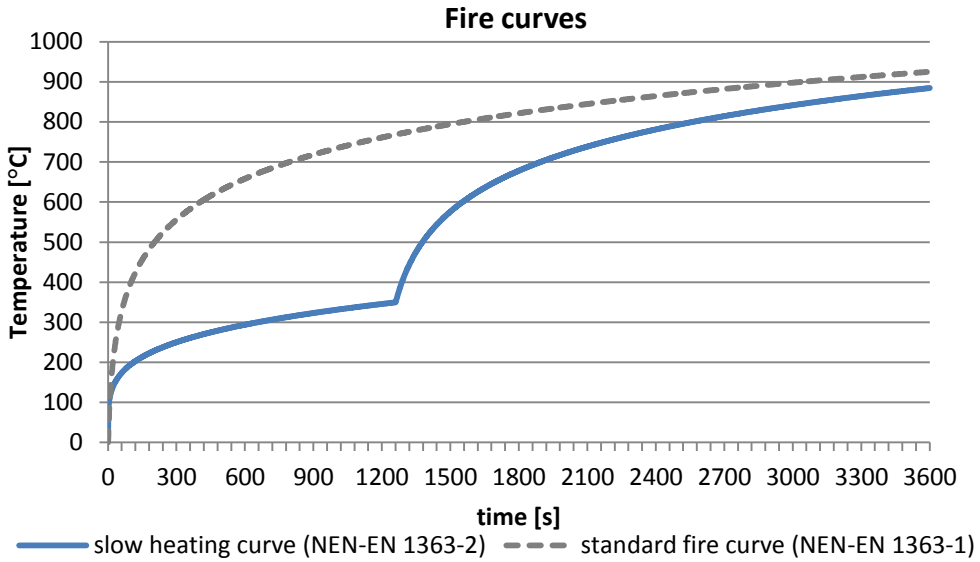

Figure 8: slow heating curve in relation to standard fire curve

Equation 15 defines the slow heating curve for the first 21 minutes, hereafter it is defined by equation 16.

for $0 < t \leq 21$ (min): $$T = 154t^{0,25} + 20 \quad (15)$$

for $t > 21$ (min) : $$T = 345 \log_{10}(8(t - 20) + 1) + 20 \quad (16)$$

The gas temperature inside the fire furnace was monitored with nine fixed plate thermocouples. Local gas temperatures inside the fire furnace have a tolerance margin of 100 °C relative to the averaged temperature curve. In addition, the percentages of glass fallout will affect the gas temperature inside the fire furnace. The surface temperatures were recorded with the use of thermocouples. The studies by Keski-Rahkonen (1988), Emmons (1988), and Pagni and Joshi (1991) have addressed the temperature difference as parameter to assess glass breakage. In addition the experimental studies by Roby, and Beyles (1991), Pagni and Joshi (1991), and Shields et al (2005) assessed the glass temperature, and the temperature differences in relation to glass breakage. This approach is taken as basis for the positioning of the thermocouples on the glazing assembly. The thermocouples were located on the inner and outer pane for all windows at the upper shaded area, and the central glass surface. The calculated temperature difference is based on the difference between these two temperatures. Additionally an infrared camera and a video camera were used to record the fallout of glass. Table 2 gives an overview of the measured temperatures with respect to their specific location.

Symbol	Thermocouple	Position illustrator
T_s	Shaded Temperature	
T_g	Glass surface temperature	
ΔT	Temperature difference	

Table 2: temperature measurements

Figure 9 gives the experimental setup for the glazing assembly with double glass before the moment of the fire experiment. Figure 10 gives the assembly with triple glazing.

Figure 9: experimental setup double glazing

Figure 10: experimental setup triple glazing

The fire furnace complies with the minimal requirements of the NEN 6069. The fixed plate thermocouples which are used for the gas temperature inside the fire furnace have a measuring range of 10 °C to 1300 °C with a maximum measuring uncertainty of ± 15 °C. The thermocouples for the shaded and surface temperatures have a measurement range between the 10 °C to 500 °C with a maximum measuring uncertainty of respectively plus minus 3 °C. The inner envelope of the fire furnace consists of lightweight refractory bricks which must have the properties as defined by equation (17) according to the NEN 6069.

$$(\lambda \cdot \rho \cdot C_p)^{0.5} \leq 600 \qquad (17)$$

The properties for lightweight refractory bricks according to the product information from Promat indicate a density of 800 kg/m^3, a specific heat capacity of 1180 J/kgK, and a thermal conductivity of 0.24 to 0.35 W/mK. Appendix III presents the properties of the refractory bricks in more detail. These properties comply with the requirements from the equation.

2.3 Experimental results

The experimental results are discussed in detail in appendix II. This report gives a complete overview of all measurement results and individual measured temperatures. The results, as discussed in this paragraph, are restricted to the research question, and will only give a summary of the results in relation to glass fallout.

2.3.1 Local gas temperatures in the fire furnace

The results for the gas temperature inside the fire furnace are presented for the upper and lower layer as illustrated by figure 11. Figure 12 gives the local gas temperature distribution for the sample with double glass near the large windows inside the fire furnace. After approximately 800 seconds and later, some slight fluctuations can be seen in the temperature as a result of small glass fallout. Figure 13 gives the gas temperature for the triple glazing assembly inside the fire furnace at the lower section. After approximately 1400 seconds and later major glass fallout disrupts the increase in temperature in the fire furnace, which in turn causes fluctuations and lower temperatures.

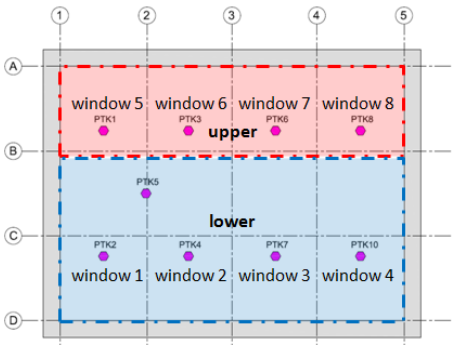

Figure 11: division of gas temperature

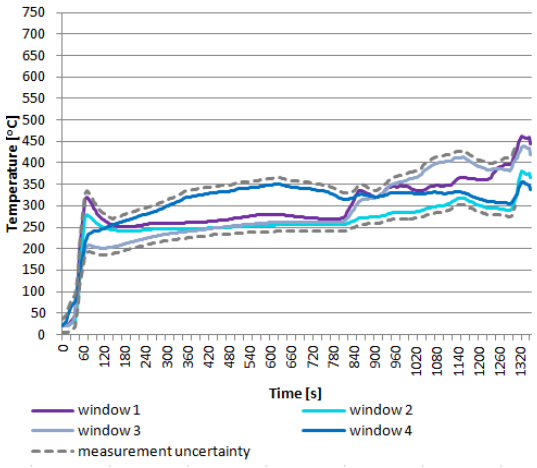

Figure 12: lower local gas temperatures in the fire furnace for the sample with double glazing

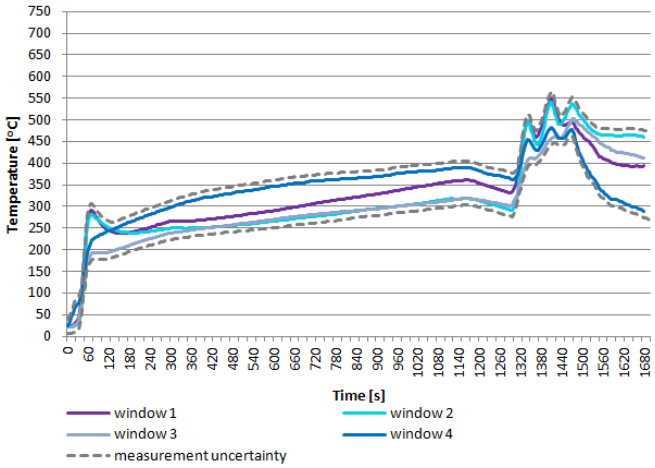

Figure 13: lower local gas temperatures in the fire furnace for the sample with triple glazing

Figure 14 gives the local gas temperatures for the double glazing assembly near the small windows inside the fire furnace. It can be seen that the major glass fallout in window 7 after approximately 1000 seconds affects the gas temperature directly. As a consequence the temperature shows a local decrease at that particular time. Contrarily for the temperature near window 6, which increases due to the inlet of oxygen. Figure 15 gives the local gas temperature for the triple glazing assembly, which shows no disruption in temperature before 1260 seconds. The deviation between the temperatures appears to be relatively small.

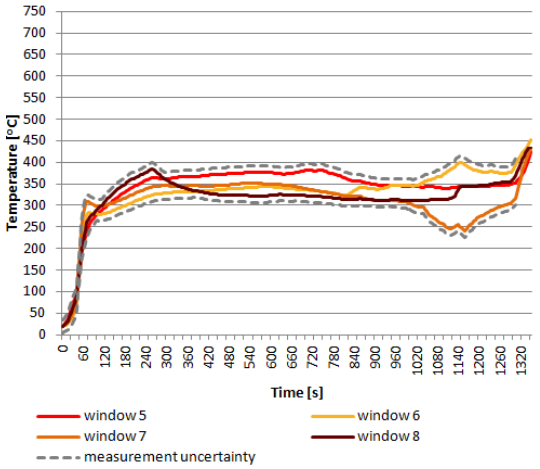

Figure 14: local gas temperatures in the fire furnace for the sample with double glazing

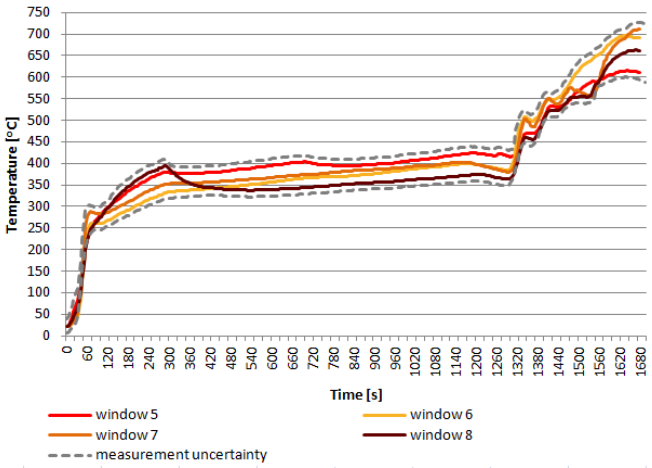

Figure 15: local gas temperatures in the fire furnace for the sample with triple glazing

Figure 16 gives the average gas temperature for the upper and lower layer of the double glazing assembly. The gas temperature between the upper and lower layer show a distinctive difference, which supports the necessity to split the upper and lower layer. Figure 17 shows more or less the same pattern for the difference between the upper and lower layer in gas temperature for the triple glazing assembly. After approximately 1500 seconds the deviation between the upper and lower gas layer will increase significantly due to major glass fallout.

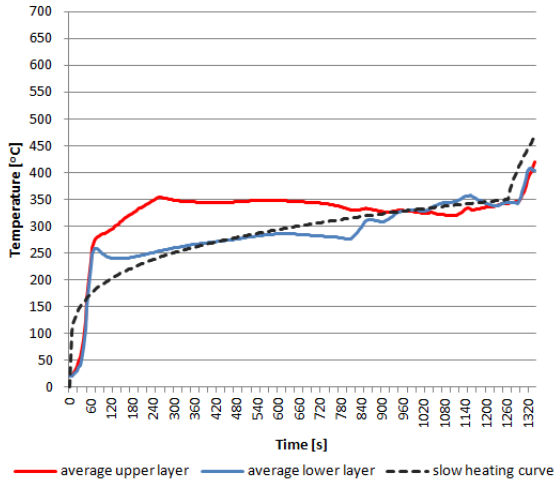

Figure 16: average gas temperature for the double glazing assembly

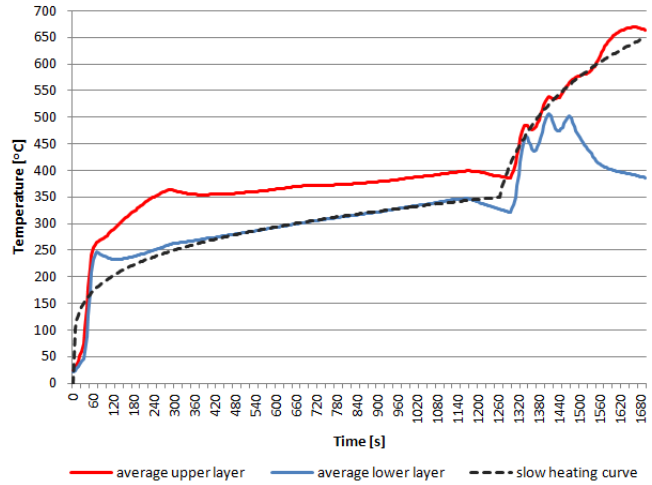

Figure 17: average gas temperature for the triple glazing assembly

2.3.2 Comparison of the temperature development in the glazing assembly

Figure 18 indicates that the averaged shaded temperatures for the assembly with double and triple glazing lay relatively close together on the inner pane. The difference in temperature between the large and small windows is higher, as a consequence of the difference in the upper and lower gas layer temperature inside the fire furnace. Figure 19 presents the shaded temperatures of the outer pane, which fluctuate more due to the difference in glass fallout and glazing system. The averaged shaded temperatures in the assembly with triple glass are consistently lower than the averaged shaded temperatures for the assembly with double glass.

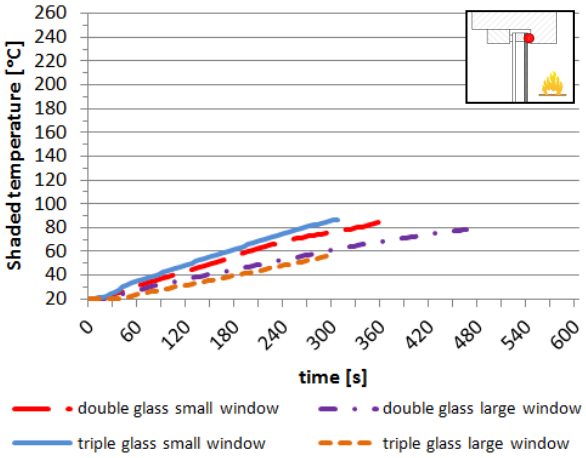

Figure 18: averaged shaded temperatures for double and triple glass on the inner pane

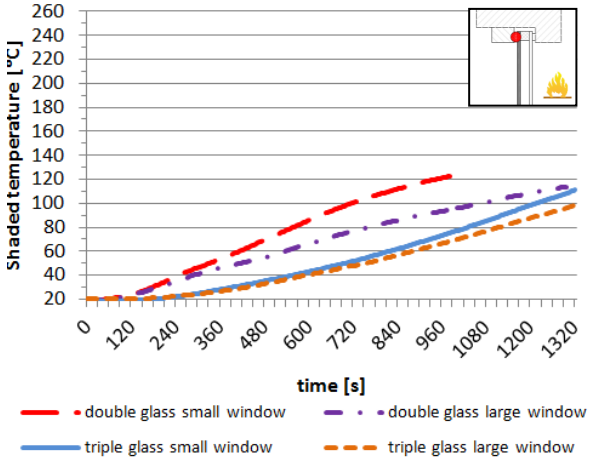

Figure 19: averaged shaded temperatures for double and triple glass on the outer pane

Figure 20 presents a comparison of the averaged glass surface temperatures on the inner side for double and triple glass. One can recognize that the glass surface temperatures between triple and double glass are almost similar during the first 300 seconds for both the small as the large windows. Figure 21 gives the averaged glass surface temperatures for the outer pane. It can be recognized that the averaged glass temperatures of triple glass are consistently lower than the averaged glass temperatures of double glass. This can be explained by the shielding effect of the inner and middle pane. Additionally, the coating will contribute to lower temperature on the outer pane, because it will reflect a part of the radiation. The averaged glass surface temperatures for the triple glass assembly on the outer pane for the smaller windows are lower than the large windows, despite the higher gas temperature in the upper layer. This is not the case for the double glazing assembly, where the temperatures of the smaller windows on the outer pane are higher than the large windows. This difference confirms that the small window with triple glass will shield a larger part of the heat than compared to the larger window.

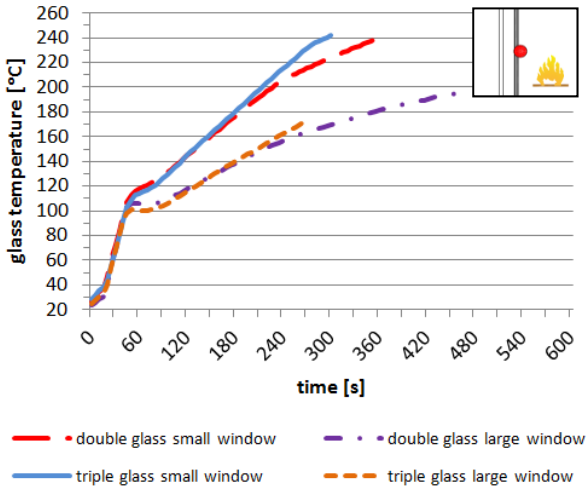

Figure 20: averaged glass surface temperatures for double and triple glass on the inner pane

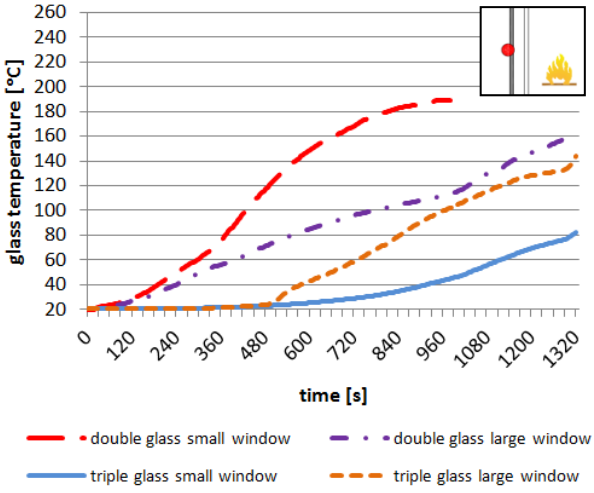

Figure 21: averaged glass surface temperatures for double and triple glass on the outer pane

Figure 22 gives the averaged temperature difference as a function of time for both glazing assemblies on the inner pane. These temperature differences between the two assemblies show the same pattern and lay relatively close together. Figure 23 gives the averaged temperature differences for the outer pane, where the deviation fluctuates highly.

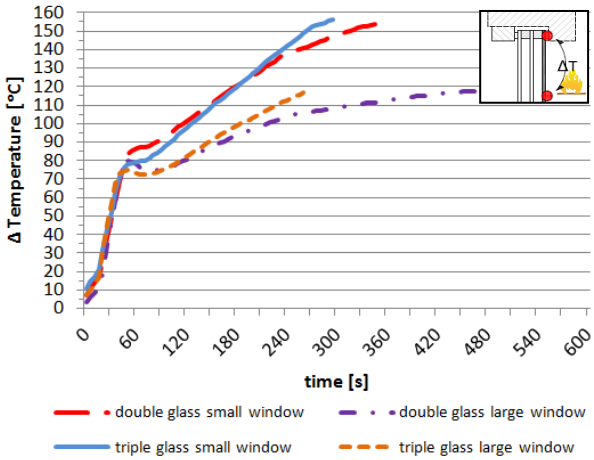

Figure 22: averaged temperature difference for triple and double glass on the inner side

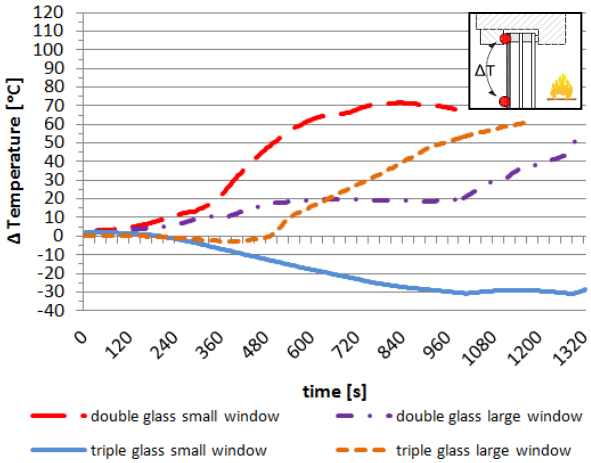

Figure 23: averaged temperature difference for triple and double glass on the outer side

2.3.3 Comparison of glass fallout

The percentages of glass fallout are based on a visual estimation from the video footage and the infrared images. During the experiment it was observed that the initial cracks started at an early stage in the fire experiment (within 1 minute). The majority of the cracks originated at the corners of the glass. The initial cracks in a specific glass section progressed in length and severity over time. Based on the same observation it could be seen that the argon gas within the cavity escaped evenly when the cracks were sufficiently wide, which expressed itself by a white haze on the window. Glass fallout occurred when multiple cracks overlapped each other. The inner panes of the triple glass tended to fallout earlier when compared to the double glazing. Contrarily, the outer panes of triple glass tended to fallout later than the outer panes of double glazing. The loss of integrity increased significantly after 21 minutes for both cases when the fire curve increased in severity. Figure 24 gives an overview of the glass areas that experienced fallout on the outer pane. The time is indicated in minutes with the notation (MM:SS).

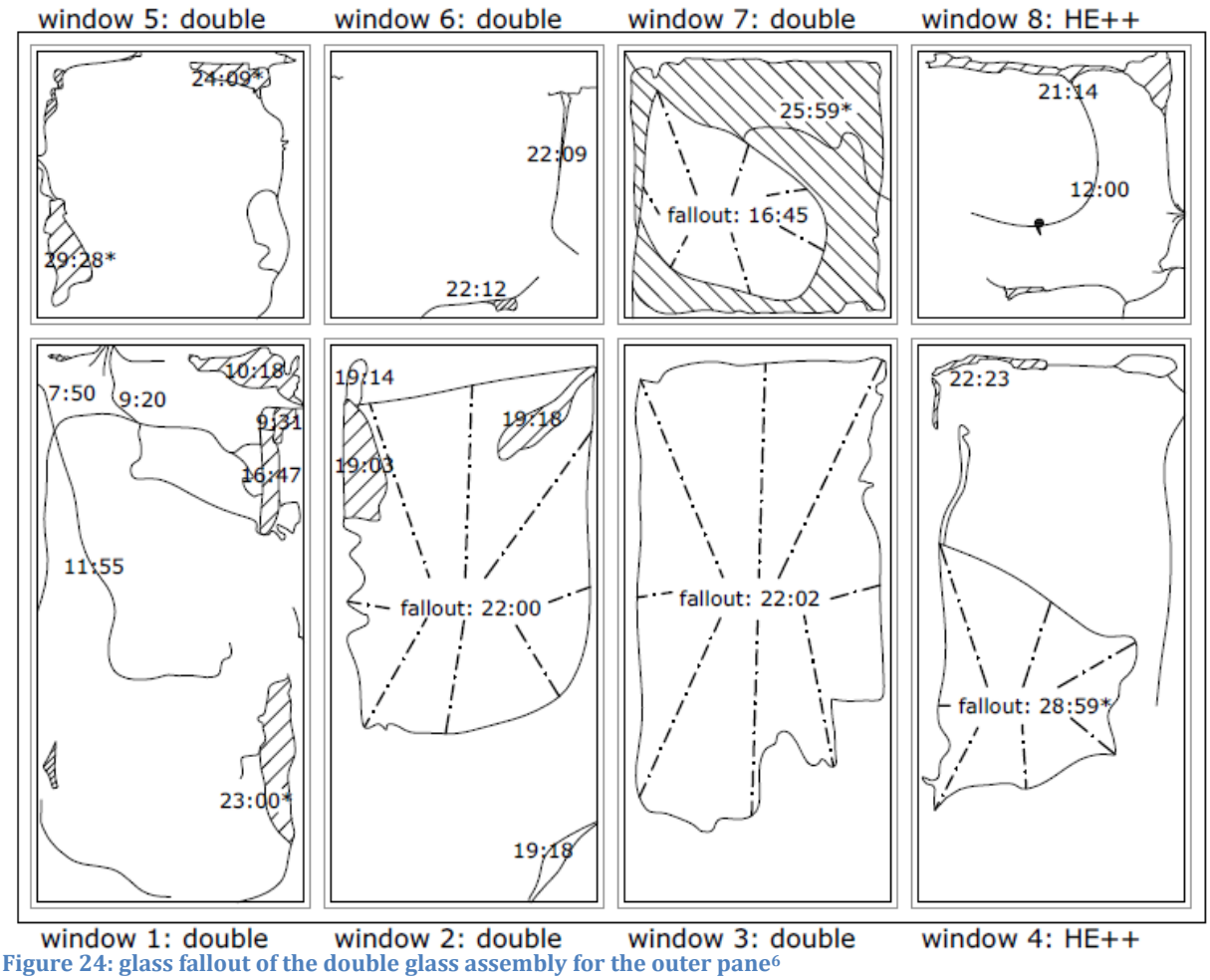

Figure 24: glass fallout of the double glass assembly for the outer pane[6]

Table 3 gives an overview of the results from the experiment with double glazing for each individual window.

Window number	1	2	3	4	5	6	7	8
Type	Double	Double	Double	HE++	Double	Double	Double	HE++
Time to first crack [s]	110	81	70	72	55	66	58	70
Time to fallout [s]	-	1320	1322	-	-	-	1005	-
Glass temperature at fallout [°C]	-	188.6	158.6	-	-	-	193.6	-
Max outer pane [°C]	158.9	188.6	158.6	125.2	273.8	187.6	199.0	264.8
ΔT at fallout	-	78.3	52.0	-	-	-	74.1	-
Max ΔT [°C]	25.0	78.3	52.0	11.8	113.5	35.6	98.3	140.6
Min ΔT [°C]	-11.8	0.0	-107.1	-43.8	-35.2	-31.7	0.0	-12.4

Table 3: results for the assembly with double glazing

Figure 25 gives an overview of glass areas which experienced fallout over time for the triple glass sample with the same notation in minutes (MM:SS).

[6] The time indication before glass fallout is indicated with a * symbol when it occurred during the cooling phase.

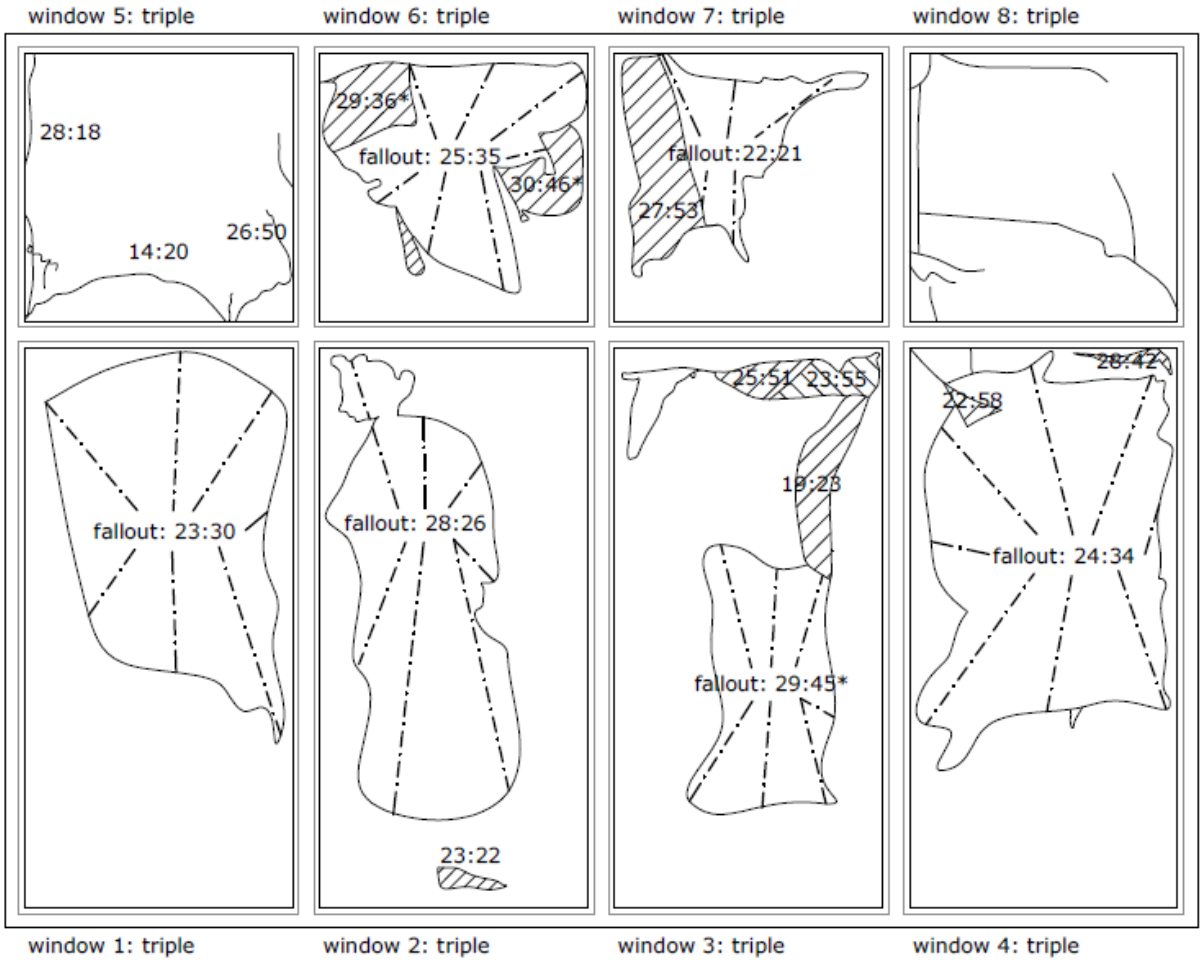

Figure 25: glass fallout of the triple glass assembly for the outer pane[7]

Table 4 gives an overview of the results from the experiment with double glazing for each individual window.

Window number	1	2	3	4	5	6	7	8
Type	Triple	Triple	Triple	Triple	Triple	Triple	Triple	Triple
Time to first crack [s][8]	n.a.	n.a.	55	n.a.	76	56	51	n.a.
Time to fallout [s]	1410	1708	-	1474	-	1535	1341	-
Glass temperature at fallout [°C]	168.0	202.0	-	168.1	-	82.7	143.2	-
Max outer pane [°C]	168.0	203.2	184.1	168.1	223.1	82.7	145.3	221.1
ΔT at fallout	n.a.	25.9	-	45.7	-	-101.1	34.8	-
Max ΔT [°C]	16.1	78.3	14.4	45.7	29.3	0.3	36.6	44.7
Min ΔT [°C]	-15.8	-6.1	-17.7	-13.8	-29.2	-101.1	-18.3	-44.8

Table 4: results for the assembly with triple glazing

Table 5 gives the average percentages of glass fallout at some specific times for both the double as the triple glazing assembly.

[7] The time indication before glass fallout is indicated with a * symbol when it occurred during the cooling phase.
[8] The time before the first crack could not be retrieved for all windows (indicated with n.a.) based on the visual judgment.

	Average fallout of double glass		Average fallout of triple glass[9]	
Time [mm:ss]	Large windows [%]	Small windows [%]	Large windows [%]	Small windows [%]
0:00	0.0	0.0	0.0	0.0
10:00	0.3	0.0	0.0	0.0
15:00	1.0	0.0	0.0	0.0
20:00	1.0	0.0	1.7	0.0
21:00	4.3	12.7	1.7	0.0
22:26	48.7	13.0	1.7	8.3
25:00	-	-	40.8	8.3
28:50	-	-	41.7	29.7

Table 5: Percentage of fallout in relation to time

2.4 Discussion

2.4.1 Differences in the gas temperature

Figure 26 presents a comparison of the difference in the averaged gas temperature inside the fire furnace between both experiments for the upper and lower layer in relation to the slow heating curve as reference. It can be concluded that the deviation between the temperatures is relative small at the initial phase (until 600 seconds). After 600 seconds the difference in the upper layer will increase. This can be partly explained by glass fallout in the double glazing assembly. One can recognize that the differences between the lower gas temperatures of the sample with double and triple glass remains relatively small. Considering the difference in the upper layer it is important to assess the fallout of both assemblies in respect to their own gas temperature during the experiment.

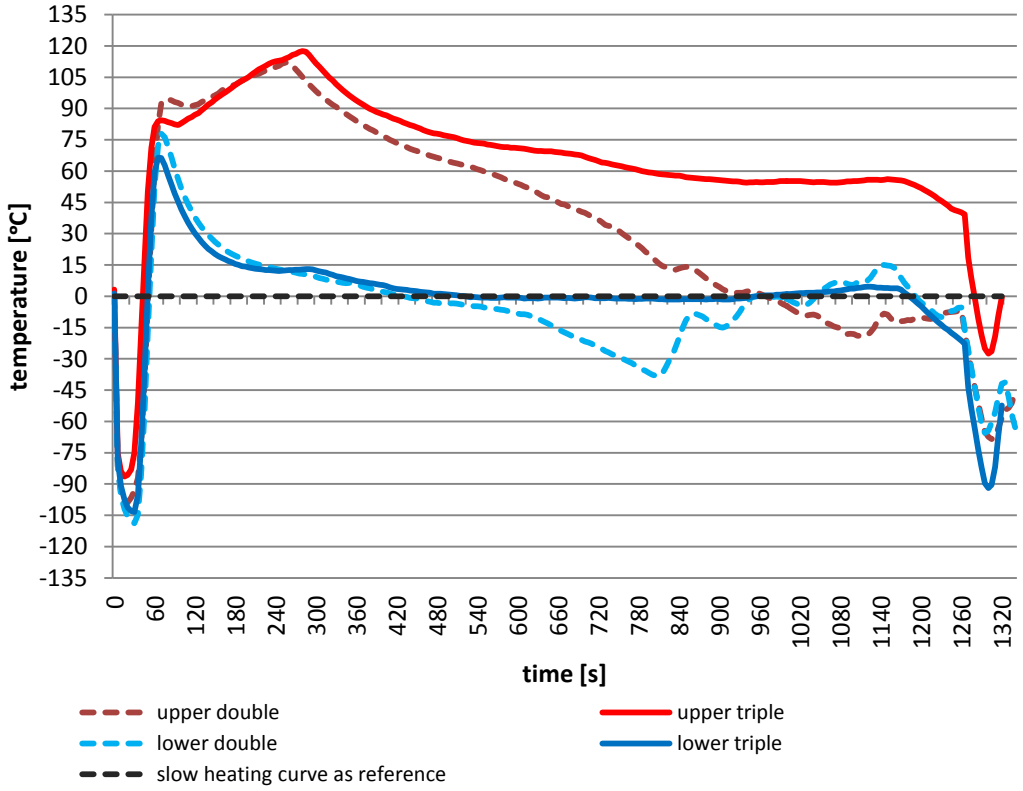

Figure 26: difference between the averaged gas temperatures

[9] The average fallout of triple glass is based on the three windows with the largest portion of glass fallout at the earliest moment in time to provide the same ratio as obtained by the average of double glass.

2.4.2 Comparison to other literature

Several studies have attempted to establish a criterion for the prediction of glass fallout for single glazing. The stress equation provided by the study of Keski-Rahkonen (1988) and Emmons (1988) gives 80 °C as the critical level where breakage occurs. The study by Pagni (1991), on the other hand, defines a maximum temperature difference of 60 °C before the occurrence of catastrophic glass failure or glass fallout. The experimental investigation by Skelly et al (1991) discusses both criteria, but describes a theoretical temperature difference of 70°C as lower limit for glass fallout to occur. The experiments indicated a higher temperature difference of 90°C. The difference between the experimentally found temperature and the theoretical temperature is explained by the direct radiation on the thermocouples, which in turn causes a temperature deviation. The study by Shields et al (2002) established some potential engineering correlations based on their experimental results of single glazing, regarding to the first crack and loss of integrity. The used correlations were gas temperature, incident heat flux, and rate of heat release. According to the experimental research of Shields et al (2001), the glass temperature at the moment of catastrophic failure of the glass (fallout) will lie in the region of 110 °C. When the criteria are compared to experimental studies with single glazing, one can recognize that the derived criteria seem to be somewhat conservative. This might be due to the fact that the given criterion is designed as a global guidance for input in a simulation, therefore it will give a worst-case scenario. Although this worst-case scenario might be preferable from the perspective of fire safety in relation to fire spreading, it does not provide a realistic approximation for the moment of an oxygen inlet through a window to the enclosure fire. A more extensive approach for the prediction of glass fallout of single glazing during fire is provided by the work of Hietanami (2005), which is based on a predetermined amount of successive cracks. The first fracture can be predicted relatively accurate with the help of the well-validated BREAK1 algorithm, established by the work of Pagni & Joshi (1991). Successive breaks are more difficult to predict, because the first crack will influence the response to heat and reduces momentarily the mechanical stresses in the glass. The average glass temperature before the occurrence of the initial crack seems to be relatively stable according to Hietaniemi (2005), (between the 78 °C and 80 °C). Glass fallout is assumed after five successive breaks. However, other studies which are addressed according to Hietaniemi (2005) define three to seven successive breaks as criterion, depending on the chosen boundary conditions.

Only a few studies have made an attempt to assess the performance of multi-pane glazing in regard to glass fallout during fire. The transmitted radiant energy for multi-pane glazing, both double and triple, are reported in the experimental study by Klassen et al (2006). The transmitted energy remained below 25% and 10% respectively. However, the composition of the glass and the glass types are entirely different from the current supply on the market. This makes a comparison of the present glazing assembly under consideration impossible. The studies by Shields, Silcock, and Flood (1998), and Shields et al (2005), which are taken as basis for the experimental rig, do assess double glazing which could be expected in conventional dwellings. Although approximately the same dimensions of glass are maintained, the experimental rig is highly different which makes a straight-forward comparison difficult. The reference results are derived from a full-scale fire experiment, which include steep thermal gradients over the vertical surface. These steep gradients do not occur in a fire furnace experiment. Also the composition of the detail is different, in terms of another materialisation and another shading thickness. The experimental research by Shields, Silcock, and Flood (1998), indicated that double glazing, although considerably weakened, remained relatively long intact. These results can only give temperature conditions which did not lead to glass fallout at best. The glass surface temperature did not exceed 450 °C, and the temperature difference did not exceed 160 °C. The second experimental study of double glazing by Shields et al (2005) established a relationship between the time before the first crack and glass fallout. However, these results do not provide a criterion which can be used as guideline for the moment of glass

fallout, and thus an inlet of oxygen for an enclosure fire. Furthermore, the statement that double glazing performs much better than single glazing in regard to integrity, i.e. a barrier for fire break out, is not quantified. In practice there will also be a strong vertical temperature gradient present during a typical enclosure fire. Although a straight-forward comparison of the experiment with the fire furnace and the reference study seems inappropriate, it can be used to explore the influence of this gradient on glass fallout. Table 6 gives a comparison between both results, where the percentages of glass fallout are mentioned with their specific times.

	HRR [kW]	Glass fallout [%]	Time [s]	Glass fallout [%]	Time [s]
Shields et al (2005) [10]		**Small upper window**		**Large window**	
Pan fire size 600	286	0	end	0	end
Pan fire size 700	466	5	540	5	877
Pan fire size 800	691	1	455	0	end
		2	638		
Pan fire size 900	1223	2	330	2	305
		5	335	5	404
		-	-	30	485
		-	-	55	1156
Pan fire size 1000	1229	5	268	55	254
		10	276	-	-
		80	688	-	-
		90	726	-	-
Fire furnace experiment[11]		**Small upper window**		**Large window**	
Window 7	510	37	1020	-	-
Window 2	450	-	-	1	600
		-	-	3	660
		-	-	6	1020
		-	-	7	1140
		-	-	80	1320

Table 6: Comparison between the experiment and the study by Shields et al (2005) for double glazing

The pan fire size of 0.6 m x 0.6 m and 0.7 m x 0.7 m shows the closest similarity to the experiment in terms of the hot gas layer. The hot gas layer of 1.0 m x 1.0 m reaches higher temperatures for a time period of 15 minutes, which are more similar to the standard fire curve. The same correlation also applies for the glass surface temperature. The other boundary conditions which are maintained (shading thickness of 20 mm and ceramic fiber insulation on the fire side) in the reference study will have a more negative influence on the results than the maintained boundary conditions in the present study. However, when the percentages of glass fallout in relation to the time are compared, it is obvious that glass fallout is more severe during the experiment than the pan fire size of 600 to 800 in the reference study. Therefore the results from the experiment can be used for an estimation of the lower breaking limit during an enclosure fire, since the fire furnace provides a worst-case scenario.

2.4.3 Spreading of the temperature development for the glazing assemblies

In some cases glass fallout occurred while the temperature difference of individual windows remained relatively low (see table 3 and 4). In other cases the glass remained intact, while the temperature differences increased to relative high temperatures. The same applies for individual cases with specific glass surface temperatures. No correlations are found between individual glass fallout of windows and specific glass temperatures or temperature differences. A limitation of the temperature difference for defining glass fallout is that it does not take into account the exposure time and the temperature development. Several graphs are presented to

[10] The percentages of fallout are derived from the three combined experiments per pan fire size.
[11] The percentages of fallout are derived from the window with the largest fallout at the earliest moment in time.

quantify the spreading between the individual glass temperatures and temperature differences. Figure 27 gives the spreading between the glass surface temperatures for the inner pane. Figure 28 gives the spreading in the glass surface temperature between the same individual windows for the outer pane. The spreading in the outer pane is substantial higher than compared to the inner pane.

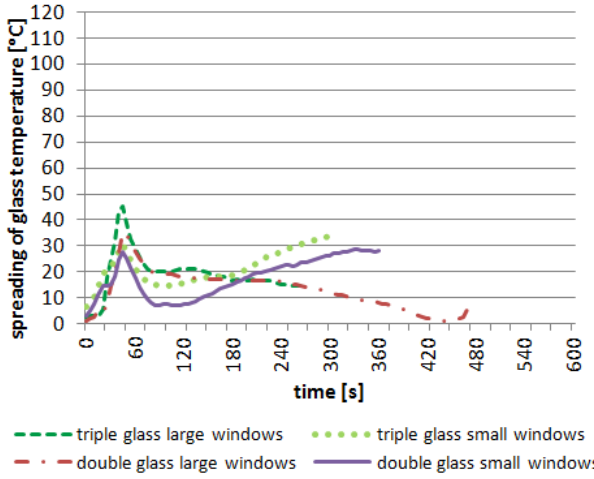

Figure 27: Spreading of the glass surface temperature on the inner pane

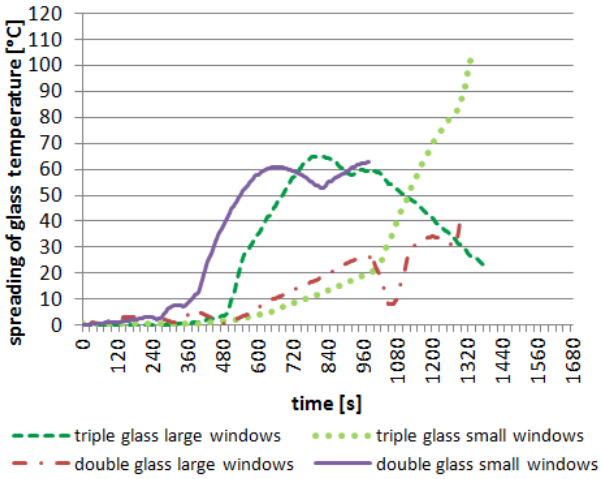

Figure 28: Spreading of the glass surface temperature on the outer pane

Figure 29 gives the temperature differences for the windows with triple glazing on the inner pane. Figure 30 presents the spreading for the temperature difference on the outer pane. The spreading for the outer pane is also substantial higher than compared to the inner pane. The spreading of both temperature differences is almost similar to the spreading in the glass temperatures.

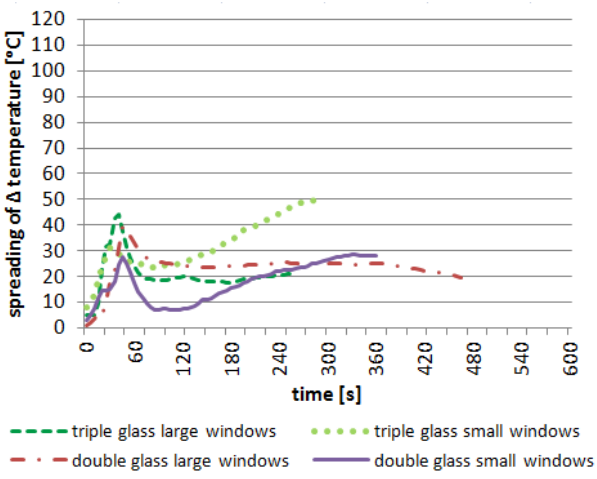

Figure 29: Spreading of the temperature difference on the inner pane

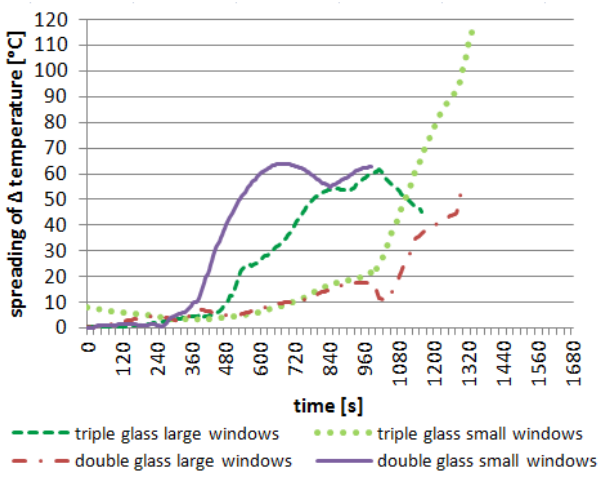

Figure 30: Spreading of the temperature difference on the outer pane

It can be acknowledged that there is a wide spreading in both glass temperatures as temperature differences between individual windows. This range can be explained by the shielding of heat by the inner pane. Also the temperature before the occurrence of glass fallout divers highly. Therefore, the glass temperature or temperature difference seem unreliable to predict glass fallout for multi-pane glazing.

2.4.4 *Engineering correlations to define glass fallout*

The averaged gas temperature in the fire furnace is not influenced by the random occurrence of glass fallout of the inner panes. Therefore a relationship between glass fallout in this study makes most sense when presented in relation to the gas temperature, and internal energy in gasvolume. Figure 31 gives the internal energy per cubic meter gasvolume in the fire furnace during the experiment with the double glazing assembly for the small windows (upper layer) and the large windows (lower layer). Figure 32 gives the internal energy per cubic meter in the fire furnace during the experiment for the triple glazing assembly.

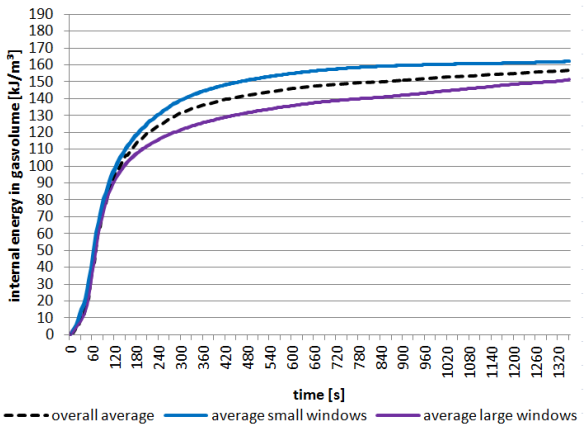

Figure 31: internal energy per m³ gasvolume in the furnace for double glazing

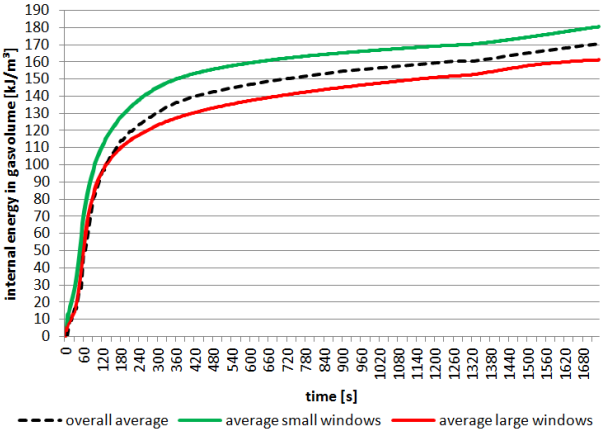

Figure 32: internal energy per m³ gasvolume in the furnace for triple glazing

Based on the experimental data a certain lower limit can be derived for the energy per cubic meter in order to increase the temperature at the inner level before glass fallout occurred during the experiment. The internal energy in gasvolume in relation to the percentage of fallout can give a working method for input of the lower limit in simulation models, provided that the heat release rate (HRR) and the peak temperatures do not exceed the given levels during the experiment. Figure 33 gives the glass fallout in relation to the internal energy in gasvolume.

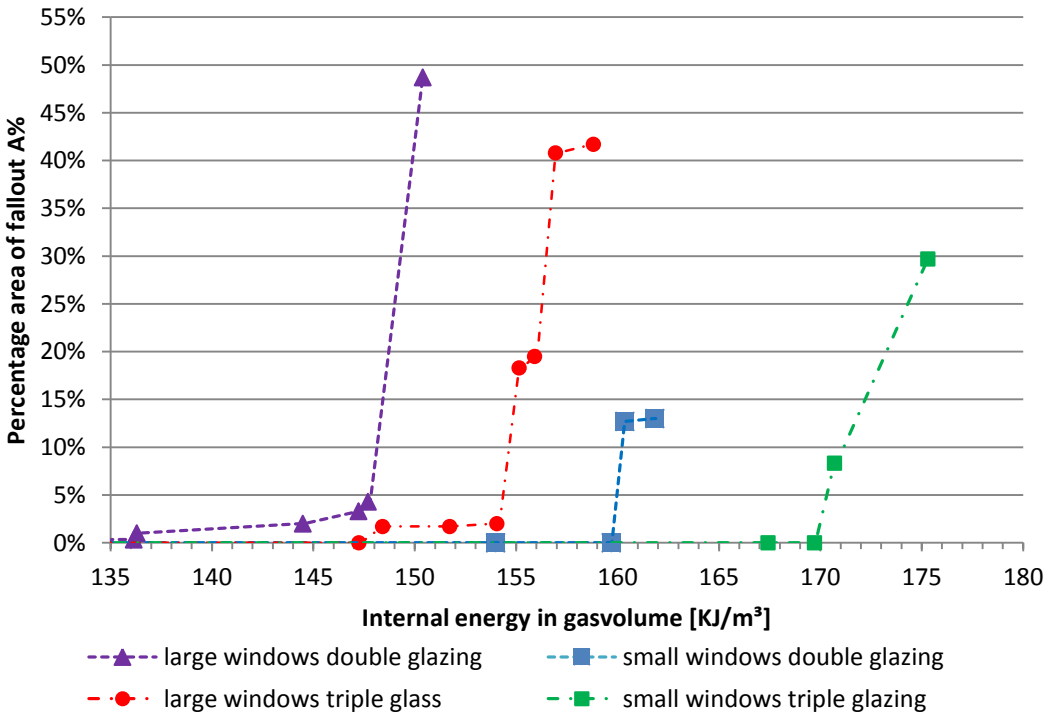

Figure 33: average glass fallout as a function of internal energy in gasvolume inside the fire furnace

There seems to be a detectable difference between the time before fallout in relation to the internal energy in gasvolume inside the fire furnace power for triple and double glass. The large windows with triple glass can endure approximately 5 kJ/m^3 more than the large windows with double glazing before major glass fallout. The difference for the small windows is approximately 9 kJ/m^3. Figure 34 gives the glass fallout as a function of the gas temperature. In this context it can be seen that the fallout of double glass occurs at lower temperatures than the triple glazing assembly.

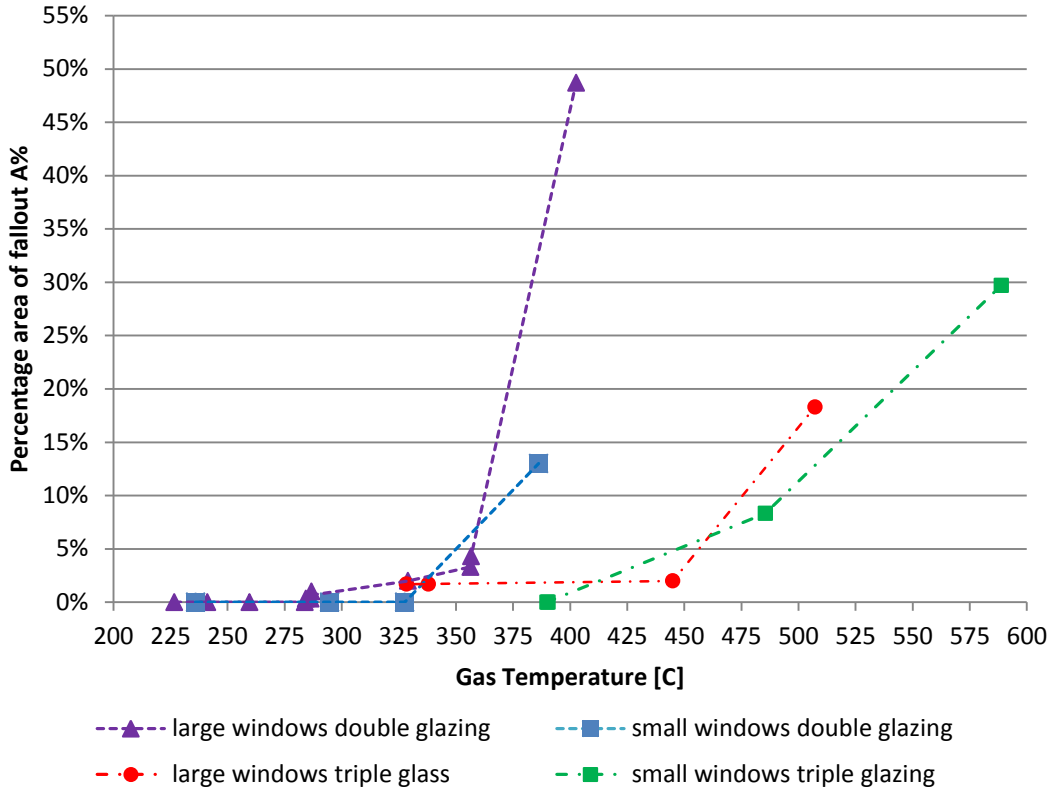

Figure 34: average glass fallout as a function of gas temperature

2.5 Conclusion based on the experimental data

The experimental results show a detectable difference between the performance of the double and triple glazing glass. The triple glazing assembly remained longer intact than the double glazing assembly, and could withstand the first part of the slow heating curve without major glass fallout. Double glass experienced small percentages of glass fallout after approximately 10 minutes, compared to 19 minutes for small percentages of glass fallout for triple glass. In both cases the percentage of glass fallout became larger as the fire intensity increased (after 21 minutes). There seems to be a relatively good agreement with the criteria for the initial crack and the experimental data at the initial crack. The spreading was relatively high between glass fallout and individual glass surface temperatures and temperature differences. At some cases the temperature difference was relatively high while glass fallout did not occur. Contrarily, glass fallout occurred in some cases at relative low temperature differences. Therefore no correlation can be found in the experimental results between the temperature difference and individual glass fallout. The various criteria for glass fallout based on the temperature difference seem too simplistic and conservative to provide a realistic time-based approach. The deviation indicates an apparent randomness in individual glass fallout, which can be explained by a large influence of imperfections in the glass and deviations during assembly. Additionally the smaller windows endured higher temperatures, while the large windows endured lower temperatures due to the difference in the upper and lower gas temperature inside the fire furnace. Therefore, a comparison of the performance makes most sense when it is expressed as a function of internal energy in the gasvolume, which takes into account the difference in temperature. This comparison indicates that the smaller windows can endure a higher internal energy in gasvolume before glass fallout occurs, when compared to large windows. The large windows of double glazing experienced no major glass fallout before approximately 147 kJ/m^3, while the large triple glass windows experienced no major glass fallout before 153 kJ/m^3. The small windows with double glazing did not experience major glass fallout before approximately 159 kJ/m^3, while the small windows for the triple glazing did not experience major glass fallout before 170 kJ/m^3. The assessment based on the averaged gas temperature in the fire furnace indicates that the double glazing assembly did not experience major glass fallout before a gas temperature of 375 ^oC. The composition with triple glazing did not experience major glass fallout before a gas temperature of 475 ^oC. Overall it can be stated that the difference in performance between the glazing systems, although detectable, might be less than originally expected. This is due to the fact that the double glass remained also relatively long intact before major glass fallout occurred.

3 Simulation

3.1 Introduction

Several simulations were conducted to support the experimental study on the performance of triple and double glass with the use of a fire furnace. The first simulation is initiated to assess the representativeness of the experiments versus an actual enclosure fire in a dwelling. This simulation consists of a calibration and an assessment on the differences. The second simulation is initiated to retrieve different fire scenarios which might occur in a dwelling in relation to the temperature rise. These results will be used for an assessment of the probability of glass fallout during an enclosure fire.

3.2 Method

Several studies have already addressed the performance of simulation programs to predict glass breakage. The simulation program BREAK1 provided by Pagni and Joshi (1991a) is suitable for a calculation of the time before the initial crack based on the temperature difference. Experimental research by Skelly, Roby, and Beyler (1991) and Pagni and Joshi (1993) validated the established program. The study by Pope et al (2007) and Dembele et al (2010), presents a probabilistic approach of the glass breakage through a simulation model. The use of a field model (FDS) to predict glass breakage is presented in the study by Kang (2008) and Qing-Song (2009). Dembele et al (2012) proposed a new simulation model based on the finite element method and assessed the influence of different edge conditions. Figure 35 gives an overview of the most suitable methods with their specific purpose.

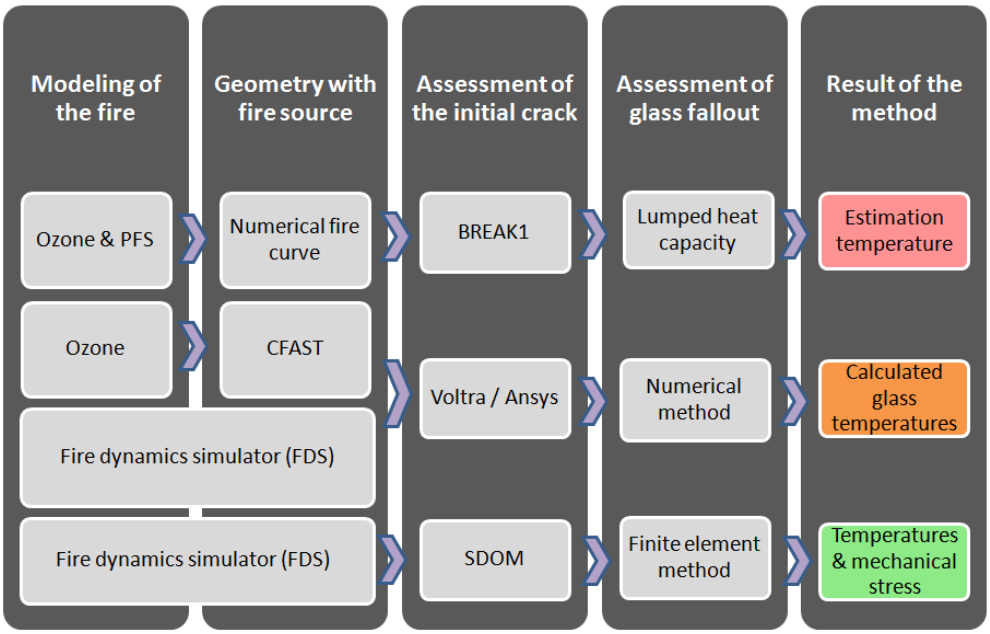

Figure 35: model approach

The first method is based on the lumped heat capacity, and presents the fastest approach, since it assumes glass fallout at the moment of the first crack. It takes only a number of boundary conditions into account. For this reason it is only suitable for simple cases or a rough indication of glass fallout during fire. The second method is based on a numerical simulation and can provide a more realistic approach of the temperatures on the glass during an enclosure fire. However, the method does not take into account thermally induced mechanical stresses. The third approach is based on the finite element method and takes into account most boundary conditions and variables into account compared to the other approaches. It can provide a method to assess both the temperatures in the glass as the mechanical stresses. Disadvantages of the method can be found in the time-consuming process and the limited available input data of material properties. Therefore the results can be unreliable. The lumped heat capacity model

is used at the initial phase to obtain an indication about the performance of glass during the experiment. The zone model is used for a stocktaking of the probability on glass fallout during an enclosure fire based on the experimental criterion of internal energy in gasvolume. The zone model will give sufficient accuracy at this time because the criterion only gives a rough estimation at best. The numerical method is used to verify the representativeness of the fire furnace to an enclosure fire in a dwelling. The detailed results which the finite element method can provide are inappropriate for a global indication, while it increases the inaccuracy and complexity. Therefore this method is not suitable for the approach in this study.

3.2.1 Numerical simulation model

The numerical simulation is initiated to retrieve the conditions during the experiment, in order to assess the representativeness of the experiment versus an enclosure fire. The simulation model is conducted with VOLTRA, version 6.0w. The model consists of a small and large window with the same dimensions as in the experiment. The used material properties are presented in appendix III, the boundary conditions and used functions are presented in appendix VII. The refractory bricks inside the fire furnace are modelled in a separate simulation model to retrieve the radiant part of energy during the experiment. Subsequently, the established radiant energy is used as input for the temperature curve as a consequence of radiation. The measured temperatures of the gas temperature at window 2 are used as input for the convective lower and middle layer. The measured upper gas temperature at window 6 is used as convective temperature curve for the small window. Figure 36 gives an impression of the model and the maintained grid. The calibration is based on a comparison of the simulated temperatures between the experimental measured temperatures on the central part of the glass for the inner and outer pane, and on the upper shaded temperature for the outer and inner pane. The comparison of the simulation model between the experimental results will be used to validate the indoor conditions in the fire furnace. The simulation will take into account stationary material properties, transient material properties, two radiation temperatures, and a range of convective heat transfer coefficients. Table 7 gives an overview of reasonable assumptions during an enclosure fire and the conditions during the experiment. Additionally the maintained variables are mentioned for the simulation model. The assembly with triple glazing is not simulated, since the glass fallout of the inner pane occurred at an early stage in the experiment. These conditions associated with glass fallout cannot be taken into account with the present simulation method.

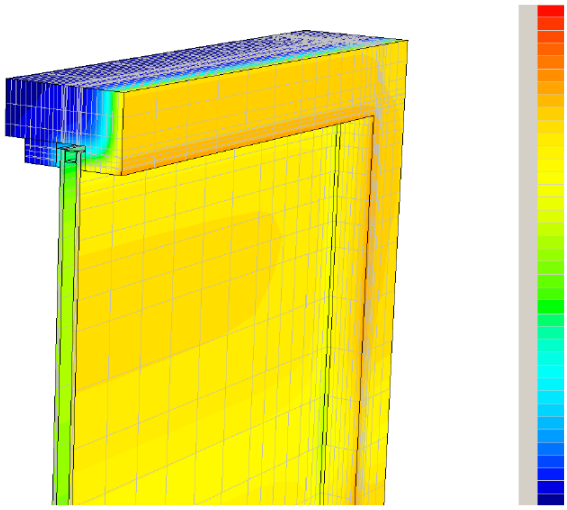

Figure 36: impression of the model

	Material properties	Radiation	h_c [W/m^{2}K]
Enclosure fire	transient	soot particles (Q_{rad}=Q_{conv})	25
Experiment	transient	refractory bricks and flames	unknown
Simulation model	stationary/transient	Q_{rad}=Q_{conv}/refractory bricks	15/ 25/35

Table 7: comparison of conditions during an enclosure fire, the experiment, and the simulation

3.2.2 Description of the Zone model

The simulations are conducted with the use of OZone version 2.2.6. The study by Spijkerboer, N (2012), and Cornil et al. (2012) already established some key parameters which will have a large influence on the fire scenario. Based on these studies, variables are selected for the assessment of the fire situations, which consist of two volumes, two compositions, and four fire scenarios'. Additionally the possibility of an open door on the inside is taken as variable. This scenario takes also into account that a window might be open. Table 8 gives an overview of the maintained dimensions for these rooms.

	Length [m]	Width [m]	Height [m]	Surface [m^2]	Volume [m^3]
Living room	6.57	7.87	2.6	51.7	134.4
Sleeping room	3.0	5.0	2.6	15.0	39.0

Table 8: composition of the construction

Table 9 gives an overview of the composition of the maintained constructions.

	Floor	Envelope	Ceiling
Light construction	Light concrete 80 mm Normal concrete 150 mm Insulation 150 mm	Board 15 mm Insulation 200 mm Brick 100 mm	Board 15 mm Insulation 200 mm Board 15 mm
Heavy construction	Light concrete 80 mm Normal concrete 150 mm Insulation 150 mm	Brick 100 mm Insulation 150 mm Brick 100 mm	Light concrete 50 mm Normal concrete 200 mm

Table 9: composition of the construction

Table 10 gives the maintained input values for the severity of a fire derived from NEN-EN 1991-1-2/NB.

Scenario	local fire	Normal fire	Rapid fire	Intense fire
Fire growth rate [s]	600 (slow)	300 (medium)	75 (ultra fast)	150 (fast)
RHR [kW/m^2]	100 (low)	250 (normal)	250 (normal)	500 (high)
Fire Load (80% fractile) [MJ/m^2]	870	870	870	870

Table 10: Input values for the simulation of the fire

Table 11 gives an overview of the area of glass surface present in the simulation models. No variations were made in the glass surface to constrain the variables to an acceptable level.

	Small windows	Large windows	Glass surface	percentage[12]
Living room	5	2	7.78 m^2	15.1 %
Sleeping room	1	1	2.61 m^2	17.4%

Table 11: opening by mean of a window

The simulation rapport of OZone can be found in appendix V, which gives the input of the geometry and boundary conditions in more detail.

3.3 Simulation results

The simulation with BREAK1, as presented in appendix IV, provides some insights on the time before the initial crack in case of a fire according the slow heating curve compared to the standard fire curve.

[12] Percentage of glass in relation to the user surface area (according to Dutch building code $\geq$ 10%)

3.3.1 Calibration of the model with double glazing

A calibration of the simulation is performed in order to verify the indoor boundary condition inside the fire furnace during the experiment. Appendix VIII gives the results for all variables which are mentioned in table 7. The simulated temperatures in the comparison, as presented in this paragraph, are based on transient material properties and a convective heat transfer coefficient of 25. Figure 37 gives a comparison of the glass temperature for the large window. In this variant the radiant heat is similar to the convective heat. Figure 38 presents the same comparison for the shaded temperatures. There seems to be a reasonable agreement between the glass surface temperatures. This is not the case for the shaded temperatures, where the simulated temperatures are consistently higher for both positions.

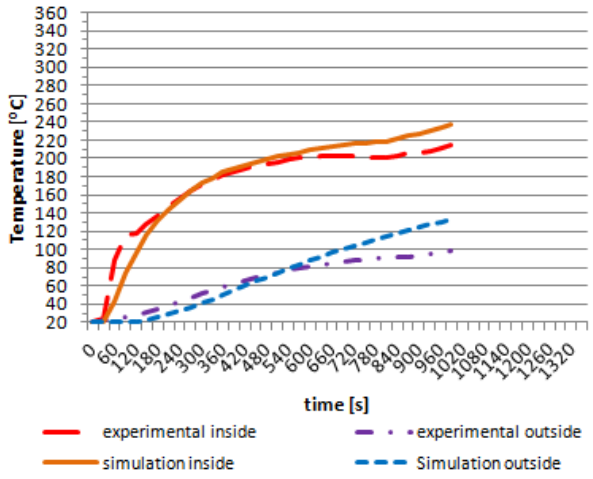

Figure 37: comparison of glass temperatures for the large window (with $Q_{rad}=Q_{conv}$).

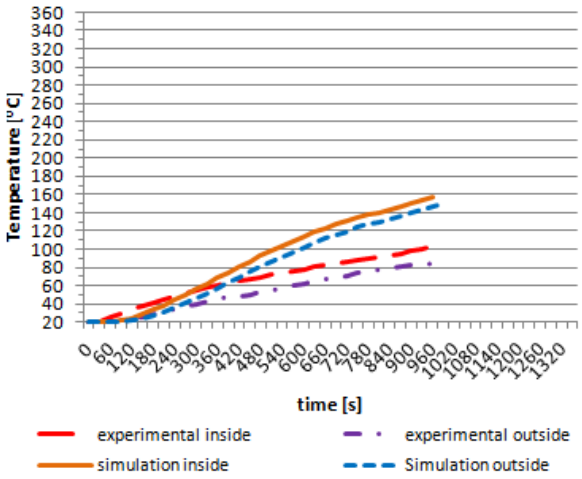

Figure 38: comparison of shaded temperatures for the large window (with Qrad=Qconv).

Figure 39 gives the comparison of the glass temperatures with the similar properties for the small window. Figure 40 gives the comparison of the shaded temperatures for the same small window. The simulated glass temperatures become increasingly higher after approximately 600 seconds compared to the experimental results. The same pattern can be seen for the shaded temperatures.

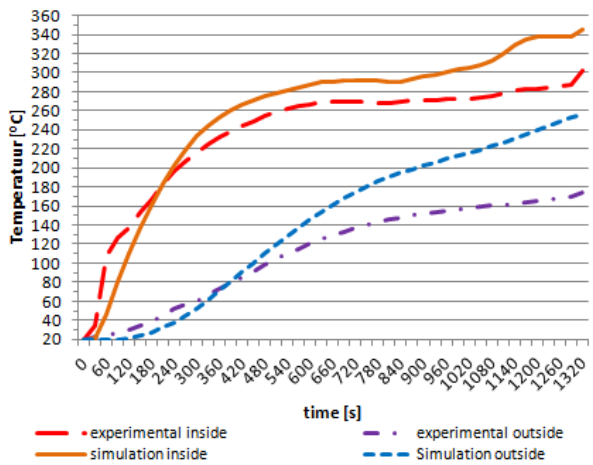

Figure 39: comparison of glass temperatures for the small window (with $Q_{rad}=Q_{conv}$).

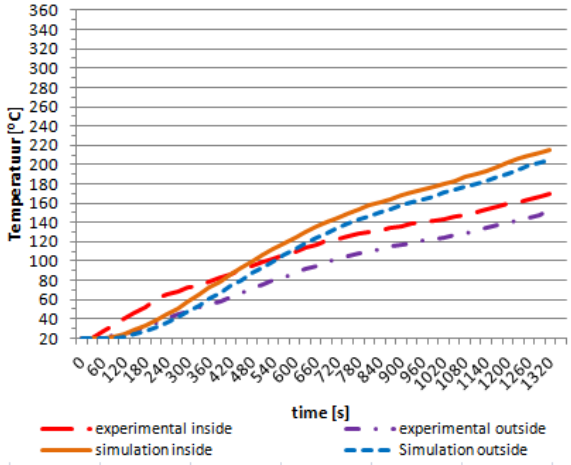

Figure 40: comparison of shaded temperatures for the small window (with $Q_{rad}=Q_{conv}$).

The simulations, with the assumption of the same convection as radiation, results in higher temperatures when compared to the experiment. A more realistic approach is expected to be achieved through the use of the transient material properties combined with the radiation

derived through the refractory bricks from the back wall. However this approach neglects the radiation from the direct flames. Figure 41 gives a comparison under these conditions between the numerical simulation and the experimental results of the glass surface for the large windows. Figure 42 presents the same comparison for the shaded temperatures in the large window. One can recognize that the simulated glass temperature on the inside remains consistently lower. The other temperatures show a better agreement with the experimental temperatures.

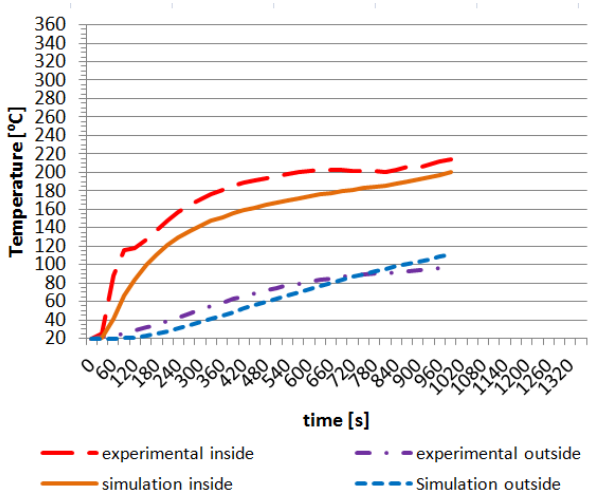

Figure 41: comparison of glass temperatures for the large window (with Q_{rad}=refractory bricks).

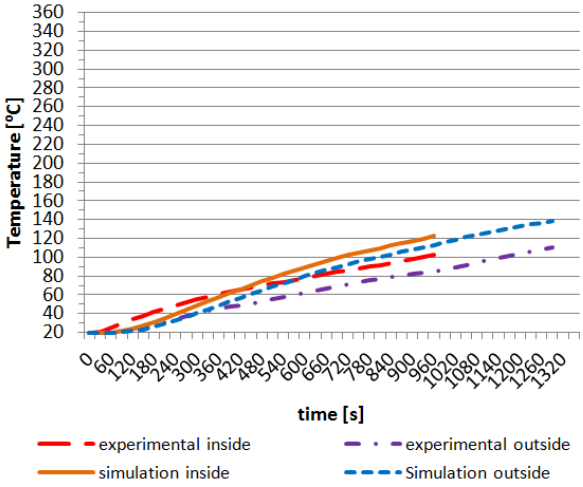

Figure 42: comparison of shaded temperatures for the large window (with Q_{rad}=refractory bricks).

Figure 47 gives the same comparison between the glass temperatures for the small window. Figure 44 gives the comparison for the shaded temperatures in the small window. It is obvious that all simulated temperatures are consistently lower than compared to the experimental temperatures. The difference is even larger for the inner glass temperature.

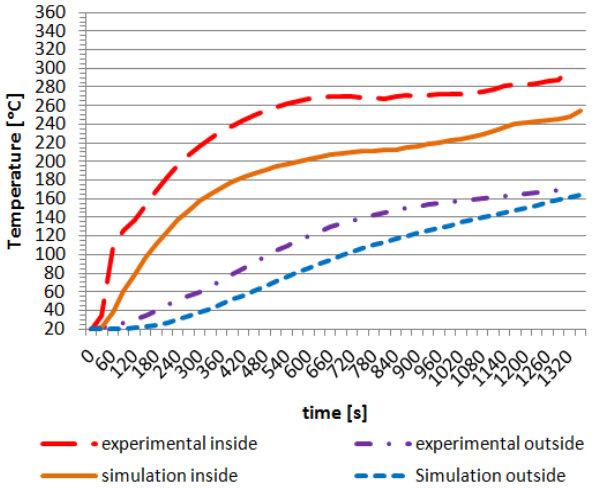

Figure 43: comparison of glass temperatures for the small window (with Q_{rad}=refractory bricks).

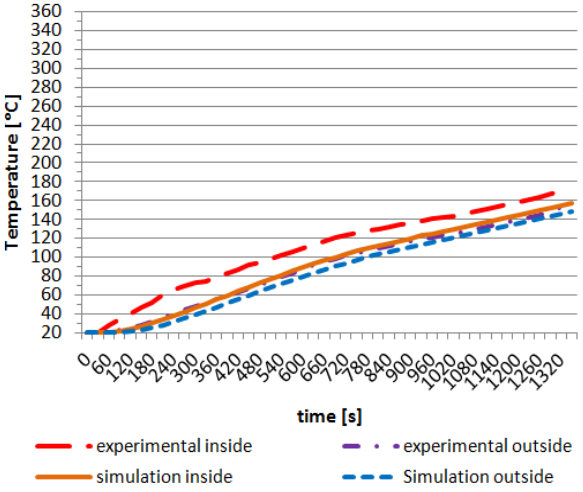

Figure 44: comparison of shaded temperatures for the small window (with Q_{rad}=refractory bricks).

3.3.2 *Fire Scenarios profiles*

Based on a zone model different temperature profiles were obtained under various boundary conditions. The various fire scenarios are presented in relation to the gas temperature layers as found in the experiment. When the temperatures of the simulated situations exceed the temperatures during the experiment, it becomes impossible to assess the potential glass fallout. This is due to the fact that the behaviour of glass with respect to fallout is not assessed for temperatures which are higher than the experimental gas temperature in the upper and lower layer. Figure 45 gives the temperatures in the living room with a heavy construction without openings. Figure 46 gives the temperatures as a result of the open door scenario under the same boundary conditions. The temperatures during a local and a medium fire for the living room with a heavy construction remain below the experimental temperatures. The rapid and intense fire exceed the temperature of the lower layer, which could mean that the large windows might experience glass fallout from that point onwards.

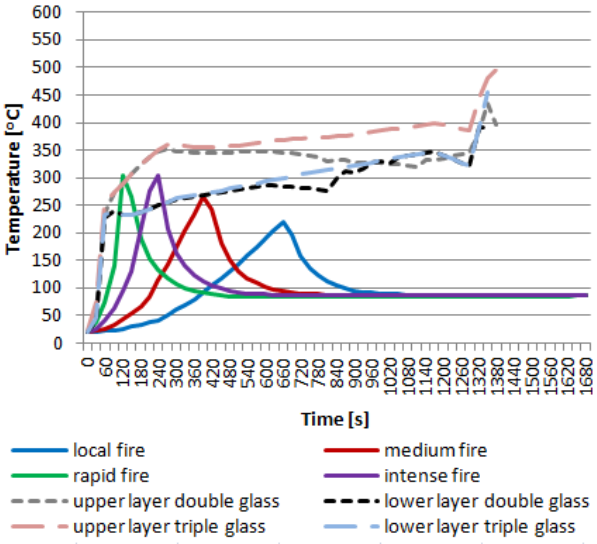

Figure 45: temperatures living room; heavy construction with closed doors

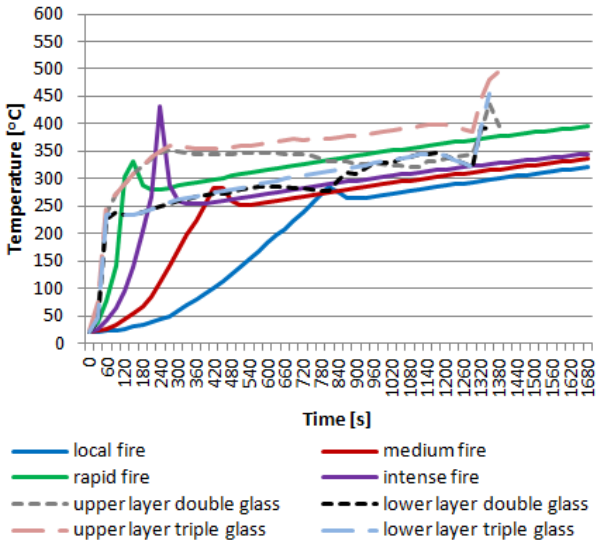

Figure 46: temperatures living room; heavy construction with opened doors

Figure 47 gives the temperatures in the living room with a light construction in relation to the experimental temperatures without openings. Figure 48 gives the temperatures for the open door scenario. The temperature during the intense and the rapid fire both exceed the experimental temperature for all experimental gas temperatures. The medium and local fire, on the other hand, will mostly remain below the temperatures which occurred during the experiment. The behaviour of glass will probably be more similar for these situations, than compared to the intense and rapid fire.

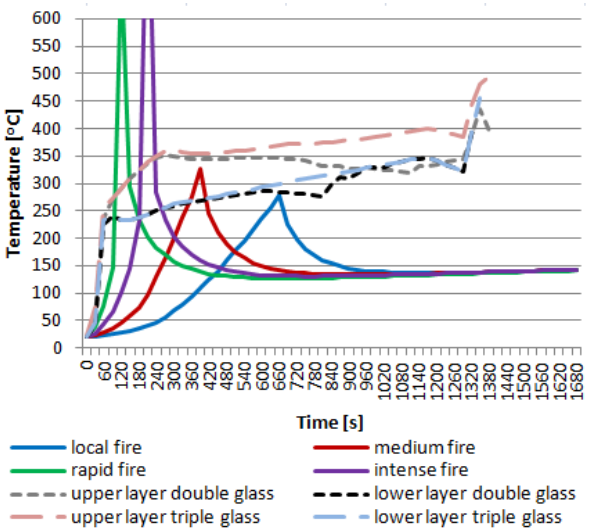

Figure 47: temperatures in the living room with a light Construction for different fire scenarios

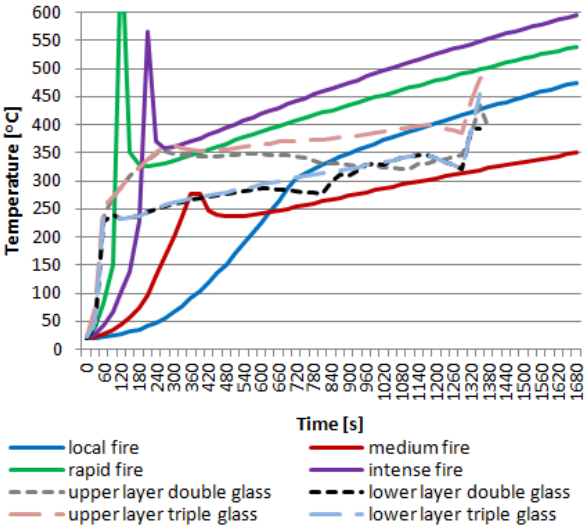

Figure 48: temperatures in the living room with a light Construction for different fire scenarios

Appendix VI presents the simulation results for the scenarios in a bedroom, where broadly the same patterns apply. The temperatures during a medium and local fire remain mostly under the temperatures measured during the experiment, while the intense and rapid fire exceed the temperatures measured during the experiment.

3.4 Discussion

3.4.1 Representativeness of the simulation model

Consistent deviations remain present between the simulated temperatures and the experimental results. These deviations can be caused by numerous factors. Part of the deviation can be explained by the input of the material properties. An increase in temperature will have an influence on the specific heat and the thermal conductivity of materials and gases. Most material properties that are used during the experiment could be retrieved in relation to this change over temperature. The properties of Argon gas are also retrieved, however this data only applies as long as the cavity does not experience loss of integrity. From the moment of the first crack onwards, the argon gas will escape and evaporate. The properties of the cavity will change to a cavity with air. Since almost all initial cracks occurred within one minute, it makes more sense to model the cavity with the boundary condition (BC_free), although this will result in somewhat higher temperatures than during the experiment. When glass fallout of the inner pane occurs, the cavity will largely disappear, and the properties will change significantly. This situation is impossible to simulate. Therefore the simulation model can only be used before the moment of glass fallout of the inner pane. The influence of the cracking and small glass fallout on the temperature is not taken into account by the simulation model. The absorption of glass is, as discussed in the theoretical section, dependent on the temperature. As a consequence the reflection and transmission properties are also transient over the temperature, since the reflection, absorption, and transmittance must be in balance. These optical material properties of the glass cannot be taken into account by the simulation program. Also the maintained emissivity given by AGC (2012) is based on a stationary ambient temperature of 20 °C. The imperfections and inconsistencies in the glazing, as described in the experimental part, will contribute even further to the uncertainties with respect to the input of materials. The calibration based on the transient material properties with an equal share of radiant and convective heat indicates higher temperatures for the simulation compared to the experimental results. The higher simulated temperatures might be partly explained by a lower radiation level inside the fire furnace than is assumed in the simulation. The neglecting of the transmission will

at the same time also results in higher simulated temperatures compared to the experimental temperatures. However, the simulation which is based on the radiation from the backside of the fire furnace with the refractory bricks, result in consistently lower temperatures compared to the experiment. This indicates either a larger influence of the (in)direct flames, or by a possible higher ventilation rate during the experiment which will result in a higher convective heat transfer coefficient. Although the implementation of a convective heat transfer coefficient of 35 W/mK provide a slightly better agreement, it still does not provide a satisfying agreement.

3.4.2 Assessment of glass fallout during an enclosure fire

This paragraph compares the various simulated scenarios for the living room between the experimental glass fallout criterion for double and triple glazing based on the internal energy in gasvolume. Appendix IV gives the same comparison for the sleeping room. **Error! Reference ource not found.** gives a comparison of the fire scenarios with a heavy construction without openings. Figure 50 gives the same comparison with an open door scenario. The scenarios without any openings do not generate enough energy to exceed the criterion as found by the experiments. The rapid fire scenario with a partly opened door do exceed the maximum criterion for the large windows (both triple as double glass), which could mean that glass fallout will occur in this fire scenario. The other fire scenarios do not exceed the given maximum energy before glass fallout could be expected.

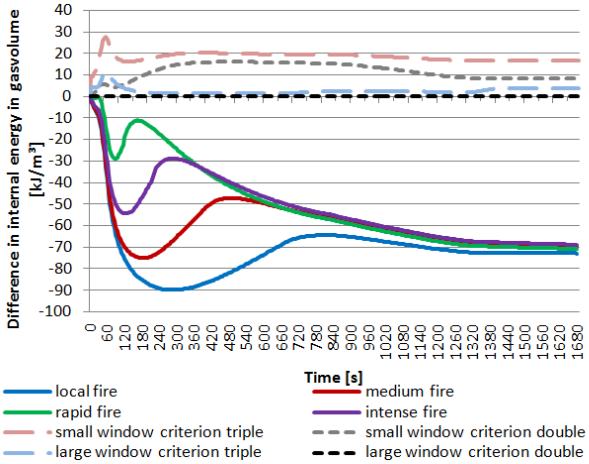

Figure 49: comparison for the heavy construction without openings.

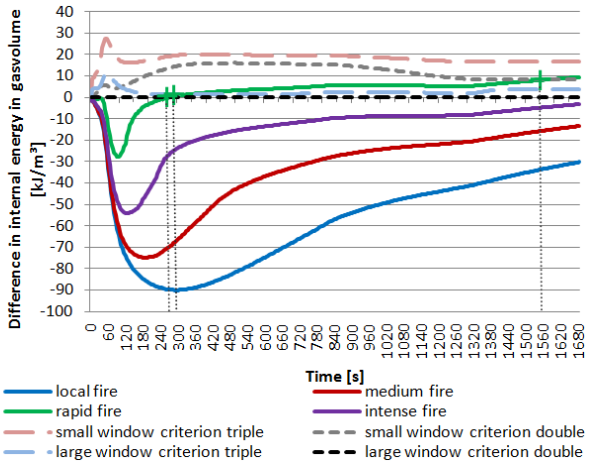

Figure 50: comparison for the heavy construction with an opened door scenario.

Figure 51 presents the same scenarios for the internal energy in gasvolume with a light construction without openings. Figure 52 presents the same comparison with an open door scenario. The internal energy in gasvolume in the scenarios without additional openings appears to be higher when compared to the heavy construction. However, they do not exceed the critical limit where glass fallout could be expected. The internal energy in gasvolume during the local and intense fire with the open door scenario do exceed the criterion for the large windows very rapidly. As time progresses, these two scenarios also exceed the criteria for the small windows. The local and medium fire with the open door scenario does not exceed the criterion for any window.

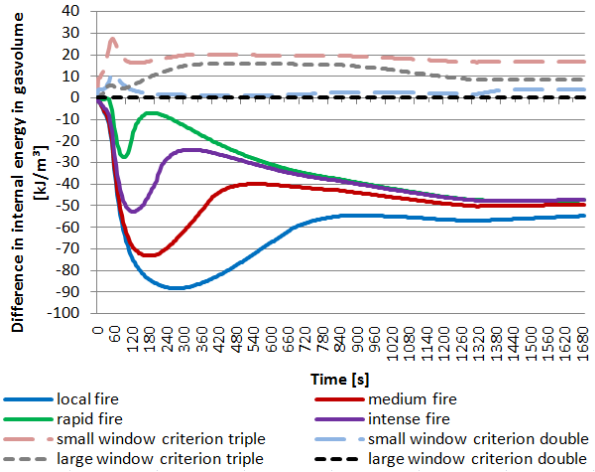

Figure 51: comparison for the light construction without openings.

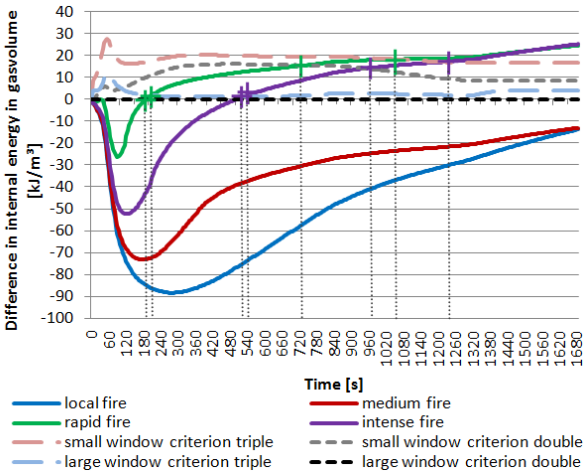

Figure 52: comparison for the light construction with an opened door scenario.

3.5 Conclusion

The calibration of the fire experiment with the numerical simulation model indicates that only a rough estimation of the temperatures can be obtained through this method. Due to the many variables such as the influence of the glass, boundary conditions of the composition, material properties, and conditions in the fire furnace it is impossible to obtain a more accurate result in the current simulation model. It seems that the results indicate a lower radiation level in the fire furnace than one would expect during an enclosure fire, however the combined heat is consistently higher than the radiation from the refractory bricks alone. Based on the current simulation model it is impossible to quantify the difference in radiation compared to an enclosure fire. Nevertheless, the found criterion as a function of internal gasvolume seems adequate for a rough estimation of glass fallout, since the combined temperatures on the inside of the glass are relatively small.

The comparison with different fire scenarios in relation to the found critical levels in the experiment indicate that a local and medium fire does not generate enough energy to cause glass fallout for both triple and double glazing. However, it seems plausible that the rapid and intense fire do generate enough energy and/or heat to cause fallout at an early stage during an enclosure fire. The detectable difference in performance of triple glazing compared to double glazing seems to make only a difference for a limited amount of situations. Furthermore the size of the window seems to be more normative than the difference between triple and double glass in relation to the fallout criteria. Finally the glass fallout seems to be more dependent on the fire scenario; as a consequence this will be most decisive whether a smouldering fire or a fully developed fire will occur. With the use of double glass, the risk on a smouldering fire scenario will be increased compared to a situation with single glass, which is known to fallout very rapidly. The risk on a smouldering fire scenario will become only slightly higher with the use of triple glazing.

4 Overall discussion

4.1 Experimental discussion

The conducted experimental research has some specific limitations and uncertainty's which will be discussed in the following paragraphs.

4.1.1 Explanation of the spreading in the experimental results

The experimental results show a large spreading with respect to the measured surface temperatures and time before the occurrence of glass fallout. Based on the experimental results no specific temperatures could be pointed out at which glass fallout occurred. The spreading suggests that other factors might also have a large influence on the moment of glass fallout than the temperature alone. Despite a careful and consistent assembly of the frame and the glass, there occurred inevitable minor differences in the composition. At some areas the glazing will have less room to expand compared to other areas in the same composition due to the manual pressure which is used by mounting the glazing bead. Additionally the glass itself is an inconsistent material which can vary within the given limits in appendix III. The possible invisible imperfections and some visible glass flakes in the glazing, contribute even further to the apparent spreading on the occurrence of the initial cracks. Individual glass fallout seems to be largely influenced by the crack bifurcation, and the crack patterns. Glass fallout will subsequently occur when various cracks overlap each other, which carve apparent random areas out of the glass pane. The glass surface temperature on the outer pane of multi-pane glazing is largely influenced by the shielded area of glass on the inner pane. As a consequence the cracks and percentage of glass fallout on the inner pane will affect the temperature on the outer pane. Other experimental research by Shields et al, (1998 to 2005) suggested that the glass fallout is also largely influenced by the severity of a fire. Due to these variables one specific temperature of the glazing or shaded area seems to be highly inappropriate to give an accurate prediction of the time before glass fallout. The criteria, as described by other literature, based on the temperature difference is therefore only applicable as a worst-case under limit as guidance for simulation interpretations for single glass, and not for multi-pane glazing.

4.1.2 Limitations of the glass fallout criterrion

The experiment is conducted with the use of the slow heating curve, which only represents a limited amount of various fire scenarios. The behaviour of the glazing assembly's might be very different when a fire will be more severe at the initial phase. The glass is expected to experience glass fallout at an earlier stage due to the increased severity. Also thermal shock could have a larger influence on the breakage of glass in this fire scenario. This information, however, cannot be obtained based on the current results. New experiments based on the standard fire curve can clarify these situations, and would therefore be a good addition. During the experiment only one composition of framing is used. An application with a plastic/aluminium frame or a composition with another shading thickness might behave completely different. The fire resistance of synthetic framing is in general assumed to be fairly short. However, experimental research is on the way, to establish the fire resistance for plastic framing with the application in passive dwellings. According to E. Boon (personal communication) these framings have a significant better fire resistance, which could mean that the same glass fallout criterion applies for this situation. Furthermore, the glazing assembly consist of a small sample size, making a statistical approach unreliable. Given the large spreading it is particularly dangerous to derive conclusion based on the used sample size. The conclusions should therefore be interpreted with a certain nuance. However, the established criterion based on the internal energy in gasvolume seems suitable to predict glass fallout within the presented boundary conditions and composition of the glazing. An advantage of the criterion is that it takes into account the window size, the

duration of the fire, and the severity of the fire. The criterion based on the gas temperature, on the other hand, provides only a maximum temperature independently on the duration of the fire. Therefore, this criterion is considered less reliable.

4.2 Discussion on the simulations

The combustion in an enclosure fire will produce smoke and soot particles, which will cause radiation on a specific surface. These conditions do not apply for the experiment with the fire furnace, where radiation only occurs due to the direct flames and the radiation from the refractory bricks. The amount of radiation as a result of the gas burners and the refractory stones inside the fire furnace is unknown, and can only be approached through a simulation at this stage. Additionally the ventilation rate inside the fire furnace was not monitored during the experiment, making it impossible to quantify. It is conceivable that the ventilation rate does not comply with the assumed heat transfer coefficient. The conditions during an enclosure fire will in practise always be turbulent, which can lead to deviations between the experimental results and an enclosure fire. The simulation apposes many uncertainties, such as the conditions of the cavity, the influence of cracks, and the limitation of the input of the optical properties of the glass. Due to all these uncertainties it is impossible to verify the radiation level inside the fire furnace.

The simulated fire profiles represent only a small range of conceivable possibilities and boundary conditions during a fire inside a dwelling. The comparison between the simulation results and the found criterion therefore serves only as an indication of the fire development under various circumstances. Various other scenarios remain possible that either will result in a ventilation controlled or in a fuel controlled fire scenario. Furthermore, it is impossible to predict the performance of glass fallout when the given temperature or internal energy in gasvolume during the experiment are exceeded by the scenario temperatures.

5 Conclusion

The conducted experiments with the use of a fire furnace have provided new insights on the performance of triple and double glazing in relation to glass fallout. The most important conclusions from this experiment are listed below:

- the fire experiments with a double and a triple glazing assembly indicated a wide spreading between the moment of glass fallout in relation to the glass surface temperature, shaded temperature, and temperature difference. Also the moment of glass fallout between individual windows seemed to occur in a random pattern. The large spreading emphasizes the influence of other break criteria such as the patterns of the crack bifurcation, inconsistencies of the glass, method of assembly by the contractor, e.g.;
- from a comparison to other reference studies one can recognize that the established criteria for glass fallout based on the temperature difference are too simplistic and conservative to provide a realistic time based approach;
- the performance of double glazing shows a detectable difference compared to triple glazing in regard to glass fallout as a function of internal energy in gasvolume and gas temperature. One must keep in mind that the given criterion is bound by several limitations. Firstly, it can only be used for a prediction of glass fallout when the gas temperature and the internal energy in gasvolume do not exceed the criterion. Additionally the experiment consists of a small sample size. Also the composition of the frame is limited to one detail. Therefore the given criterion only functions as an indicative lower limit for glass fallout.

Several simulations have been conducted to support the experimental research, which have led to the following conclusions:

- the results indicate that the radiation inside the fire furnace is less than one would expect during an enclosure fire. It is impossible to quantify the difference in radiation based on the conducted simulations. However, it is not expected to lead to an over-estimation of the criterion.
- the detectable difference in performance of double and triple glazing as found in the experimental research, only slightly influences the glass fallout. As a consequence the difference in performance will in general not cause another fire development.

Based on the combined results of the experimental investigation with the fire furnace and the simulated fire scenario profiles, it seems plausible that the risk on a smouldering fire scenario in a dwelling will increase with the application of double and triple glazing compared to a situation with single glazing. The increase in risk seems to be impossible to quantify, because it is dependable on various boundary conditions such as the size of the windows, the composition of the detail, method of assembly, and fire severity. Additionally, the fire scenario can be influenced by the occupants through variable oxygen inlets such as inner doors or outer windows (for ventilation purposes). From the perspective of fire safety engineering it is recommended to take into account both a fully developed as a smouldering fire scenario inside current dwellings.

6 Recommendations

The results of this study have raised new questions and uncertainty's which would be worthwhile to investigate. Due to the delimited scope of this study it was not possible to take into account these new questions:

- the current study does not take into account the pressure variations inside a dwelling during a fire. High overpressures that could occur in an air-tight dwelling might reduce the time before glass fallout. Therefore it is recommended to investigate the pressure differences between different types of dwelling during an enclosure fire;
- due to the scope of this study the current experiments are limited to the use with the slow heating curve. Extending the experimental research with the standard fire curve with the same glazing compositions will be a good addition. This addition will provide data to extend the found criterion to other fire situations, such as the rapid fire and the intense fire;
- When the same experiment with single glazing is performed under the same boundary conditions, it will become possible to make a quantitative comparison between the multi-pane glazing;
- The analysis of the measurement results have signalled some apparent unexplainable temperature differences in the HE++ glass compared to the double glazing. The coating might influence the measured data of the thermocouples. (comparison of double with HE++). Further analysis on this topic is omitted because it falls beyond the scope of this study;
- The representativeness of the fire furnace in relation to radiation and convective heat compared to an enclosure fire is not quantified due to the lack of time. It would be a good addition to quantify the consequence for the difference in boundary conditions. Extending the simulation with the help of SDOM would give a better prediction;

7 Figure list

References

Ades, C., Toganidis, T., Traverse, J.P., (1990). High temperature optical spectra of soda-lime-silica glasses and modelization in view of energetic applications. Journal of Non-Crystakkine Solids 125 (1990): 272-279.

Dr. ir. A.M. AbdelGhany, personal communication, 8 October 2012, National Research Center Egypt, Spectroscopy department physics division.

Arthur, E., Cote, P.E. (2008). Fire protection handbook 20th edition, Quincy: National Fire Protection Association (NFPA).

Babrauskas V. (2010). Glass breakage in fires. Fire Science and Technology Inc, 2010.

Boon, E., Smartwin, personal communication, 20 June 2012..

Bukowski R.W. et al. (2007). Performance of Home Smoke Alarms Analysis of the Response of Several Available Technologies in Residential Fire Settings. NIST Technical Note 1455-1.

Cuzzillo B.R., Pagni P.J. (1998). Thermal Breakage of double-pane glazing by fire. Journal of fire Protection engineering, 9 (1): 1-11.

Dembele S., Rosario R.A.F., Wen J.X., Wang Q.S., Warren P.D, (2010). Thermal and stress Analysis of glazing in fires and glass fracture modelling with a probabilistic approach. An international journal of computation and methodology, 58 (6): 419-439.

Dembele S., Rosario R.A.F., Wen J.X. (2012). Thermal breakage of window glass in room fires conditions – Analysis of some important parameters. Building and Environment 54 (2012): 61-70.

Dr. ir. S. Dembele, personal communication, 11 October 2012, Kingston University London, Mechanical and automotive engineering, contacted on.

Dillon S.E. (1998). Analysis of the ISO 9705 Room/Corner Test: Simulations, Correlations and Heat Flux Measurements. NIST-GCR-98-756.

Emmons H.W. (1988). Window glass breakage by Fire. Home Fire Project Technical Report No. 77, Harvard University.

Gardon R. (1958). Calculation of temperature distributions in glass plates undergoing heat treatment. J AM Ceram Soc 41.

Herpen, R.A.P. van (2007). Rookdichtheid en zichtlengte. Kennisbank bouwfysica, Fire Safety Engineering B-17.

Herpen, R.A.P. van (2012). Equivalent fire duration of a natural fire concept in comparison with the standard fire curve. Adviesburo Nieman BV.

Hietaniemi, J. (2005). Probabilistic simulation of glass fracture and fallout in fire. VTT Building and Transport, Espoo.

Kadoya, K., Matsunaga, N., Nagaashima, A. (1985). Viscosity and thermal conductiviry of dry air in the gaseous phase. Departmant of Mechanical Engineering, J. Phy. Chem. Ref. Data, 14 (4).

Kang K. (2009). Assessment of a model development for window glass breakage due to fire exposure in a field model. Fire Safety Journal 44 (2009): 415-424.

Keski-Rahkonen O. (1988). Breaking of Window Glass Close to Fire. Fire and Materials, 12: 61-69.

Khalil, E.M.A., ElBatal, F.H., Hamdy, H.M., Zidan, H.M., Aziz, M.S., Abdelghany, A.M., (2009). Infrared absorption spectra of transition metals-doped soda lime silica glasses. Physica B 405 (2010): 1294-1300.

Klassen M.S., Sutula J.A., Holton M.M., Roby R.J., Izbicki T. (2006). Transmission through and breakage of multi-pane glazing due to radiant exposure. Fire Technology, 42: 79-107.

Liming, L., Qiyuan X., Heping, Z., (2011). Evaluation of Monte Carlo method for modelling glazing behaviour during radiant exposure. Journal of Fire protection Engineering 21 (2011): 265.

Manual of Trisco and Voltra December 2009. Retrieved July 7, 2012, from http://www.physibel.be/v0n2vo.htm

NCNG Handboek voor de glasfabricage 1997

NEN 6055: Thermische belasting op basis van het natuurlijk brandconcept: Bepalingsmodel. Thermal load in a natural fire concept, 2010.

NEN 6069: Beproeving en klassering van de brandwerendheid van bouwdelen en bouwproducten, 2005.

NEN-EN 1363-1: Bepaling van de brandwerendheid – Deel 1: Algemene Eisen, 1999. Correctieblad C1, 2001.

NEN-EN 1363-2: Bepaling van de brandwerendheid – Deel 2: Alternatieve en aanvullende procedures, 1999. Correctieblad C1, 2001.

NEN-EN 1364-1: Bepaling van de brandwerendheid van niet-dragende bouwdelen – Deel 1: Wanden, 1999. Correctieblad C1, 2001.

NEN-EN 1991-1-2: Eurocode 1 - Actions on structures – Part 1-2: General actions – Actions on structures exposed to fire, 2002.

NEN-EN 1991-1-2/NB: National Annex to NEN-EN 1991-1-2, 2007.

Pagni, P.J. (1989). Fire physics; promises, problems and progress. Fire safety science: Proc 2nd Int. Symp., pp. 49-66.

Pagni P.J. & Joshi A.A. (1991a). Users' Guide to BREAK1, The Berkeley Algorithm for Breaking Window Glass in a Compartment Fire. NIST-GCR-91-596.

Pagni P.J. & Joshi A.A. (1991b). Glass Breaking in Fires. Fire Safety Science 3: 791-802.

Pagni P.J. & Joshi A.A. (1993). Fire-Induced Thermal Fields in Window Glass, I-Theory. Fire Safety Journal 22 (1994): 25-43.

Pagni P.J. & Joshi A.A. (1993). Fire-Induced Thermal Fields in Window Glass, II-Experiments. Fire Safety Journal 22 (1994): 46-45.

Parry, R., (2003). Implementation of a glass fracture module for the BRANZfire compartment fire zone modelling software. University of Canterburry, Master thesis 2003

Physics and equations for heatflow (n.d.). Retrieved October 3, 2012, from http://hyperphysics.phy-astr.gsu.edu/hbase/hframe.html

Physical properties of timber (n.d.). Retrieved November 5, 2012 from http://www.fs.fed.us/ccrc/topics/urban-forests/docs/physical%20properties%20and%20moisture%20relations%20of%20wood.pdf

Pope, N.D., Bailey, C.G., (2006). Development of a Gaussian glass breakage model within a fire field model. Fire Safety Journal 42 (2007): 366-376.

Product information AGC Thermobel glazing (n.d.). Retrieved October 16, 2012, from http://www.yourglass.com/agc-glass-europe/nl/nl/dubbele_beglazing/thermobel/brand_description.html

Product information Kerafix 2000 (n.d.). Retrieved October 4, 2012, from http://www.proflex.se/index.php?page=shop.getfile&file_id=87&product_id=61&option=com_virtuemart&Itemid=136

Product information lightweight refractory bricks, Promat 09-11-2012.

Product information refractory bricks inside the fire furnace (n.d.). Retrieved October 6, 2012, from http://www.promat-hti.be/nl/category41.htm.

Qing-song W., Yi Z., Jin-hua S., Wen J., Dembele S. (2011). Temperature and Thermal Stress Simulation of Winow Glass Exposed to Fire. Procedia Engineering 11, (2011): 452-460.

Rubin, M. (1985). Optical Properties of Soda Lime Silica Glassess. Solar Energy Materials 12, (1985): 275-288.

Shields T.J., Silcock G.W. & Flood M.F. (2001). Performance of Single Glazing Assembly Exposed to Corner Fires of Increasing Severity. Fire and Materials, 25 (4): 123-152.

Shields T.J., Silcock G.W. & Flood M.F. (2001). Performance of Single Glazing Assembly Exposed to Centre Fires of Increasing Severity. Fire and Materials.

Shields T.J., Silcock G.W. & Flood M.F. (1998) The Behavior of Double Glazing in an Enclosure Fire. Journal of Applied Fire Science, 7 (3):267-286.

Shields T.J., Silcock G.W. & Flood M.F. (2005). Behaviour of Double Glazing in Corner Fires, Fire Technology, 41 (2005): 37-65.

Skelly M.J., Roby R.J. & Beyler C.L. (1991). An experimental investigation of glass breakage in compartment fires. Journal of fire Protection Engineering, 3 (1): 25-34.

Spijkerboer, N (2012). Brandveilig wonen in een passiefhuis; een verkennen onderzoek naar de brandveiligheid in een passiefhuis. Afstudeeronderzoek Saxion Hogeschool.

Tammes, E., Vos, B.H. (1983) . Warmte-en Vochttransport in bouwconstructies. Second edition, Apeldoorn: Kluwer technische boeken B.V.

Thermal fluid mechanics (n.d.). Retrieved November 5, 2012 from http://www.isaacnewton.utwente.nl/documents/onderwijs/Samenvattingen/Bachelor/B2/SamenvattingSWO.pdf

Tiesinga, B.W., Sakonidou, E.P., Berg, van den, H.R. (1994). The thermal conductivity of argon in the critical region. Journal of Chem. Phys, 101 (8).

Wang, Q, Zhang, Y., Sun, J. Dembele, S., Wen, J. (2011). Temperature and thermal stress simulation of window glass exposed to fire.

Zeller, R.C., Pohl, R.O., (1971). Thermal Conductivity and Specific Heat of Noncrystalline Solids. Physical Review B, 4 (6).

Appendix I: Measurement protocol

Appendix II: Experimental report

Appendix III: Material properties

Properties Soda Lime Silica glass; type Planibel

Chemical composition	
SIO_2	69 to 74%
NA_2O	10 to 16%
CaO	5 to 14%
Mgo	0 to 6%
Al_2O_3	0 to 3%
Others	0 to 5%

Mechanical properties			Thermal properties		
Symbol	Parameter	Unit	Symbol	Parameter	Unit
ρ	Bulk density	2500 kg/m^3	α	Linear coefficient of expansion	$9 \cdot 10^{-6}$
E	Young's modulus	70,000 N/mm^2	C	Specific heat capacity	720 J/(kg·K)
σ	Breaking stress	45 N/mm^2	λ	Thermal conductivity Stationary (20 °C)	0.9 to 1.3 kWh/m^2
			ε	Normal emissivity	0.89
			ε_{cor}	Corrected emissivity	0.837

Kerafix 2000 properties (www.proflex.se)

Chemical composition	
SIO_2	61.0 - 67.0%
CaO	27.0 - 33.0%
MgO	2.5 - 6.5%
AI_2O_3	< 1.0%
Fe_2O_3	< 0.6%

Mechanical & Thermal properties			Thermal conductivity		
Symbol	Parameter	Unit	Temperature	Unit	
ρ	Bulk density	96 kg/m^3	20	0.06	W/mK
			200	0.06	W/mK
α	Linear coefficient of expansion	$6.0 \cdot 10^{-6}$	400	0.09	W/mK
C	Specific heat capacity	1180 J/(kg·K)	600	0.14	W/mK
			800	0.22	W/mK

Refractory bricks inside the fire furnace (www.promat-hti.be)

Chemical composition	
AL_2O_3	55
SIO_2	42
Fe_2O_a	0.6
TiO_2	1.1
$CaO + M_2O$	0.3
$K_2O + Na_2O$	1.1

Mechanical & Thermal properties			Thermal conductivity		
Symbol	Parameter	Unit	Temperature [°C]		Unit
ρ	Bulk density	800 kg/m^3	400	0.24	W/mK
σ	Breaking stress	2.4 N/mm^2	600	0.27	W/mK
α	Linear coefficient of expansion	$6.0 \cdot 10^{-6}$	800	0.30	W/mK
C	Specific heat capacity	1180 J/(kg·K)	1000	0.32	W/mK
			1200	0.35	W/mK

Glazing construction properties

Double glazing (www.yourglass.com)

Composition	
4 mm	Planibel Clear
12 mm	Argon cavity 90%
4 mm	Planibel Clear
U_g-value	2.7 W/(m^{2}K)

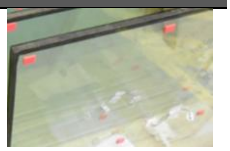

Energy properties			
Symbol	Parameter	EN410	ISO 9050
T_s	Direct Energy Transmission	72	72
ρ_r	Energy reflection	13	13
σ_a	Total energy absorption	15	15
UV	UV transmission	47	-

HE++ glazing (www.yourglass.com)

Composition	
4 mm	Planibel Clear
12 mm	Argon cavity 90%
4 mm	Planibel Top N+
U_g-value	1.3 W/(m²K)

Energy properties			
Symbol	Parameter	EN410	ISO 9050
T_s	Direct Energy Transmission	52	49
ρ_r	Energy reflection	28	30
σ_a	Total energy absorption	20	21
UV	UV transmission	21	-

Triple glazing (www.yourglass.com)

Composition	
4 mm	Planibel Top N+
12 mm	Argon cavity 90%
4 mm	Planibel Clearvision
12 mm	Argon cavity 90%
4 mm	Planibel Top N+
U_g-value	0.7 W/(m²K)

Energy properties			
Symbol	Parameter	EN410	ISO 9050
T_s	Direct Energy Transmission	41	39
ρ_r	Energy reflection	34	36
σ_a	Total energy absorption	25	26
UV	UV transmission	10	-

Appendix IV: BREAK1 simulation

The algorithm of the program BREAK1 can be used to simulate the occurrence of the initial crack in the glass during an enclosure fire. Input data which is required are the thermal conductivity, thermal diffusivity, absorption length, breaking stress, Young's modulus, linear coefficient of expansion, glass thickness, shading thickness, half width, and hot gas temperature. The program is sufficiently validated with the help of experimental studies and shows in general good resembles.

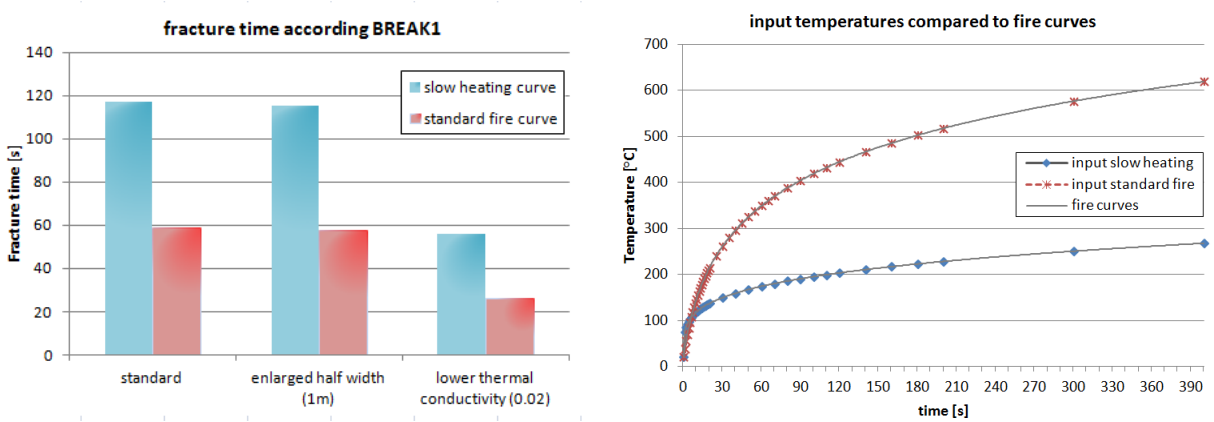

Figure 53: Comparison of fracture time based on the BREAK 1 algorithm

Figure 53 gives the result of the BREAK1 simulation, where the results for the standard fire curve are compared to the slow heating curve. The righter graph gives the input temperatures compared to the real fire curves. The input temperatures were refined until the simplification of the curve had no influence on the results. One can recognize that the single float glass can withstand the slow heating curve approximately twice as long as the standard fire curve before an initial crack occurs. Based on the results it is expected that the first crack of the glass on the inner pane will occur around the 117 seconds for the small glass and 115 seconds for the larger glass pane.

Input BREAK1 for the standard variant

Parameter	input	Influence & correlation according sensitivity analysis by VTT
Half width	0.5 m	A smaller size of the pane will lead to an improved endurance during a fire. Below a half width size of 200 mm square pane (400 mm x 400 mm), the endurance will increase strongly. The influence of larger panes size above a half height of 500mm is small. Contrarily, small planes will have less heat capacity which will lead to the opposite effect with a reduction of the endurance.
Glass thickness	4 mm	A thicker glass thickness correlates approximately linear to the gas temperature required before the occurrence of the first fracture. Thicker glass can endure higher temperatures before the initial crack occurs. The average glass temperature for a pane thickness of 2-6 mm before the initial fracture is roughly constant and starts increasing for thicker panes.
Glass thermal conductivity	0.77 W/m K	A higher thermal conductivity will improve approximately linear the ability to withstand higher gas temperatures

		before the occurrence of the initial fracture. The average glass temperature, on the other hand, remains approximately constant for the variations in thermal conductivity.
Glass thermal diffusivity	0.36·10-6 m2/s	The thermal diffusivity determines the relative distribution of the temperature. A larger thermal diffusivity implies a faster heat transfer to the backside. The same applies for a smaller thickness. The influence of changes in the thermal diffusivity are more pronounced when compared to the thermal conductivity. A lower thermal diffusivity will improve the endurance in a non-linear way before the first fracture occurs related to the gas temperature. The glass temperature before the first fracture remains relative constant with other values of the thermal diffusivity.
Glass absorption length	0.1·10-2 m	The absorption length defines the distance before the incident intensity has dropped to the penetration depth d* defined as 1/e. The glass absorption length has only a small influence on both the hot gas layer temperature and the average glass temperature at the first fracture in a glass pane.
Glass mechanical breaking stress	0.47·108 N/m^2	The glass breaking stress increases linearly when the temperature of the hot gas layer at the first fracture increases. Furthermore, also the average glass temperature increases linear at the occurrence of the first fracture as the breaking stress increases, although the influence is strong compared to other factors.
Glass Young modulus	0.7·1011 N/m^2	The Young modulus also known as the tensile or elastic modulus defines the stiffness of an elastic material. In other words it expresses a prediction to which extend a material sample extends or shortens under tension.
Glass linear coefficient of expansion	0.9·10-5 1/oC	The expanding process of a material in responds to heating is defined by the linear coefficient of thermal expansion. The lower the linear expansion coefficient of a material, the lower the induced stress field will be and consequently, the higher the temperatures required to cause the first fracture for both the gas temperature as the glass temperature. The linear coefficient of expansion has a strong influence on the endurance of the glass before an initial fracture occurs.
Shading thickness	15 mm	The shading thickness defines the impingement size of the window frame which is responsible for temperature difference between the edges and the glass pane. Shading thickness may have a strong influence on the performance on a fire resistance test of the glass. Both the hot gas layer temperature and the average glass temperature experience a steep increase for small shading thickness (below 5-15 mm depending on the glass thickness) at the first crack. The influence of the shading thickness, although notable, appears to be much weaker than the linear coefficient of expansion.

Appendix V: OZone Simulation rapport

OZone V 2.2.6 Report

Created:	3-12-2012 at 9:33:24

ANALYSIS STRATEGY

Selected strategy:	Combination 2Zones - 1 Zone Model
Transition criteria from 2 Zones to 1 Zone	
Upper Layer Temperature	≥ 500°C
Combustible in Upper Layer + U.L. Temperature	≥ Combustible Ignition Temperature = 300 °C
Interface Height	≤ 0,1 Compartment Height
Fire Area	≥ 0,5 Floor Area

PARAMETERS

Openings

Radiation Through Closed Openings:	0,8
Bernoulli Coefficient:	0,7

Physical Characteristics of Compartment

Initial Temperature:	293 K
Initial Pressure:	100000 Pa

Parameters of Wall Material

Convection Coefficient at the Hot Surface:	25 W/m²K
Convection Coefficient at the Cold Surface:	9 W/m²K

Calculation Parameters

End of Calculation:	3600 sec
Time Step for Printing Results:	30 sec
Maximum Time Step for Calculation:	5 sec
Air Entrained Model:	Heskestad

Temperature Dependent Openings

All openings activated at:	400 °C

Stepwise Variation

Temperature [°C]	% of Total Openings [%]
20	25
200	40
400	50

Linear Variation

Temperature [°C]	% of Total Openings [%]
20	10
400	50
500	100

Time Dependent Openings

Time [sec]	% of Total Openings [%]
0	0
5400	100

COMPARTMENT

Form of Compartment:	Rectangular Floor	
Height:	2,6	m
Depth:	7,87	m
Length:	6,57	m
Roof Type:	Flat Roof	

DEFINITION OF ENCLOSURE BOUNDARIES

Floor

Material (from inside to outside)	Thickness [cm]	Unit Mass [kg/m³]	Conductivity [W/mK]	Specific Heat [J/kgK]
Light weight Concrete [EN1994-1-2]	8	1600	0,8	840
Normal weight Concrete [EN1994-1-2]	15	2300	1,6	1000
Glass wool & Rock wool	15	60	0,037	1030

Ceiling

Material (from inside to outside)	Thickness [cm]	Unit Mass [kg/m³]	Conductivity [W/mK]	Specific Heat [J/kgK]
Normal weight Concrete [EN1994-1-2]	20	2300	1,6	1000
Light weight Concrete [EN1994-1-2]	5	1600	0,8	840

Wall 1

Material (from inside to outside)	Thickness [cm]	Unit Mass [kg/m³]	Conductivity [W/mK]	Specific Heat [J/kgK]
Normal Bricks	10	1800	0,7	840
Glass wool & Rock wool	15	60	0,037	1030
Normal Bricks	10	1800	0,7	840

Openings

Sill Height [m]	Soffit Height [m]	Width [m]	Variation	Adiabatic
0	2,6	0,000022	Constant	no
0	2,3	0,85	Stepwise	yes

Wall 2

Material (from inside to outside)	Thickness [cm]	Unit Mass [kg/m³]	Conductivity [W/mK]	Specific Heat [J/kgK]
Normal Bricks	10	1800	0,7	840
Glass wool & Rock wool	15	60	0,037	1030
Normal Bricks	10	1800	0,7	840

Openings

Sill Height [m]	Soffit Height [m]	Width [m]	Variation	Adiabatic
0,5	2,4	0,924	Time Dependent	no
1,376	2,3	0,924	Time Dependent	no

Wall 3

Material (from inside to outside)	Thickness [cm]	Unit Mass [kg/m³]	Conductivity [W/mK]	Specific Heat [J/kgK]
Normal Bricks	10	1800	0,7	840
Glass wool & Rock wool	15	60	0,037	1030
Normal Bricks	10	1800	0,7	840

Openings

Sill Height [m]	Soffit Height [m]	Width [m]	Variation	Adiabatic
1,376	2,3	0,924	Time Dependent	no
1,376	2,3	0,924	Time Dependent	no
1,376	2,3	0,924	Time Dependent	no

Wall 4

Material (from inside to outside)	Thickness [cm]	Unit Mass [kg/m³]	Conductivity [W/mK]	Specific Heat [J/kgK]
Normal Bricks	10	1800	0,7	840
Glass wool & Rock wool	15	60	0,037	1030
Normal Bricks	10	1800	0,7	840

Openings

Sill Height [m]	Soffit Height [m]	Width [m]	Variation	Adiabatic

0,5	2,4	0,924	Time Dependent	no
1,376	2,3	0,924	Time Dependent	no

Smoke Extractors

Height [m]	Diameter [m]	Volume [m³/sec]	In/Out
2,5	0,1	0,047	out
2,5	0,1	0,047	in

FIRE

Fire Curve:	NFSC Design Fire	
Maximum Fire Area:	51,7059	m²
Fire Elevation:	0	m
Fuel Height:	1	m

Occupancy	Fire Growth Rate	RHRf [kw/m²]	Fire Load qf,k [MJ/m²]	Danger of Fire Activation
User Defined	300	250	870	1

Active Measures

Description	Active	Value
Automatic Water Extinguishing System	No	$\delta_{n,1} = 1$
Independent Water Supplies	No	$\delta_{n,2} = 1$
Automatic Fire Detection by Heat	No	$\delta_{n,3} = 1$
Automatic Fire Detection by Smoke	No	
Automatic Alarm Transmission to Fire Brigade	No	$\delta_{n,5} = 1$
Work Fire Brigade	No	$\delta_{n,6} = 1$
Off Site Fire Brigade	No	
Safe Access Routes	Yes	$\delta_{n,8} = 1$
Staircases Under Overpressure in Fire Alarm	No	
Fire Fighting Devices	Yes	$\delta_{n,9} = 1$
Smoke Exhaust System	Yes	$\delta_{n,10} = 1$

Fire Risk Area:	12,5	m²	$\delta_{q,1} = 1$
Danger of Fire Activation:			$\delta_{q,2} = 1$
$q_{f,d}$=	696,0	MJ/m²	

Combustion Heat of Fuel:	17,5	MJ/kg
Combustion Efficiency Factor:	0,8	
Combustion Model:	Extended fire duration	

RESULTS

Fire Area: The maximum fire area (51.71m²) is greater than 25% of the floor area (51.71m²). The fire load is uniformly distributed.

Switch to one zone: Lower layer Height < 10.0% ocompartment height at time [s] 215.00

Fully engulfed fire: Temperature of zone in contact with fuel >300.0°C at time [s] 440.00

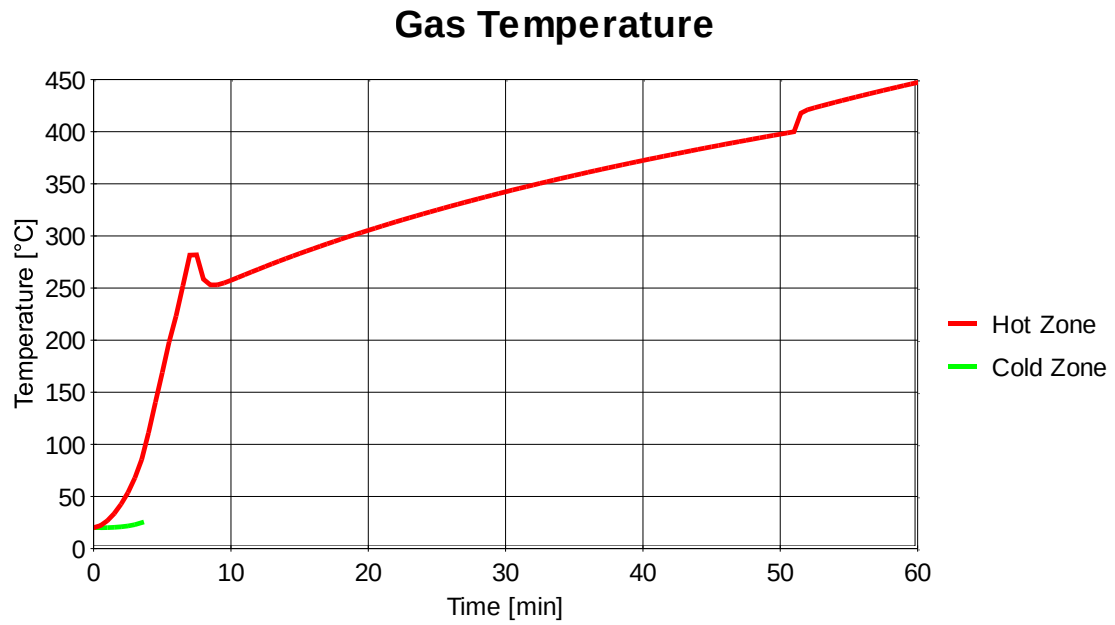

Analysis Name:

Peak: 447 °C At: 60 min

Figure 1. Hot and Cold Zone Temperature

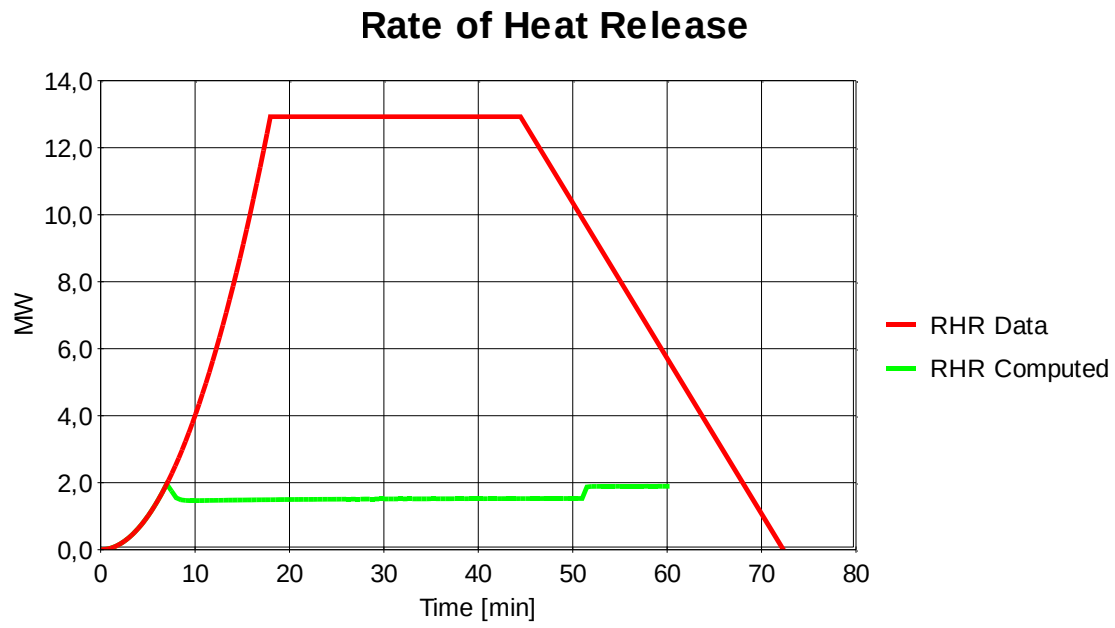

Analysis Name:

Peak: 12,93 MW At: 18,0 min

Figure 2. RHR Data and Computed

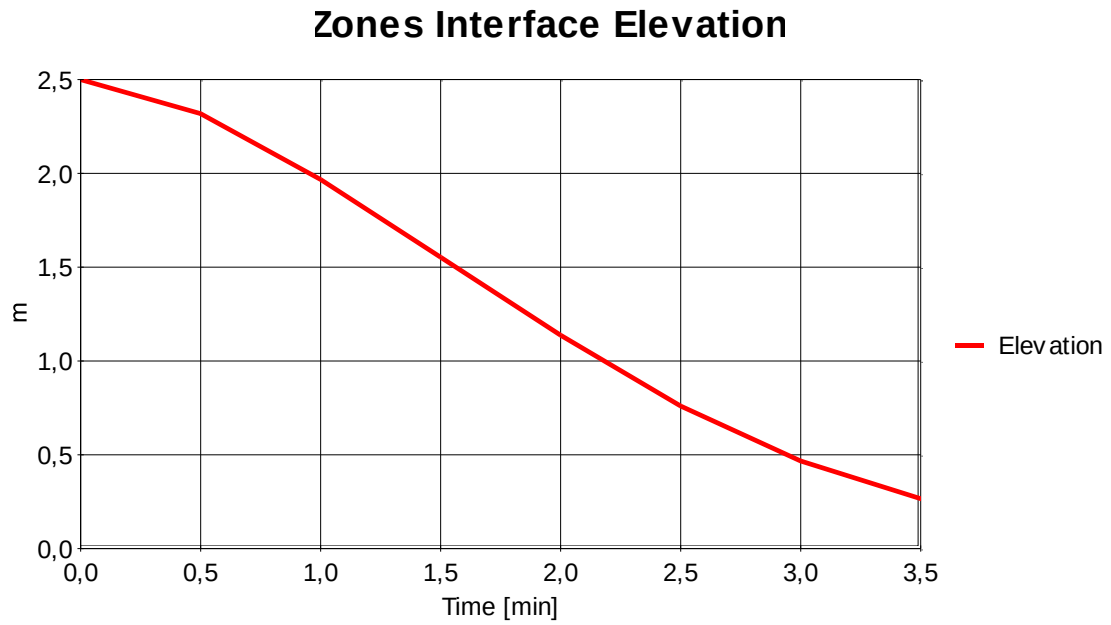

Analysis Name:

h = 0,27 m At: 3,50 min

Figure 4. Zones Interface Elevation

Appendix VI: Additional simulation results for the bedroom

Temperatures

Temperature in the bedroom with a heavy construction

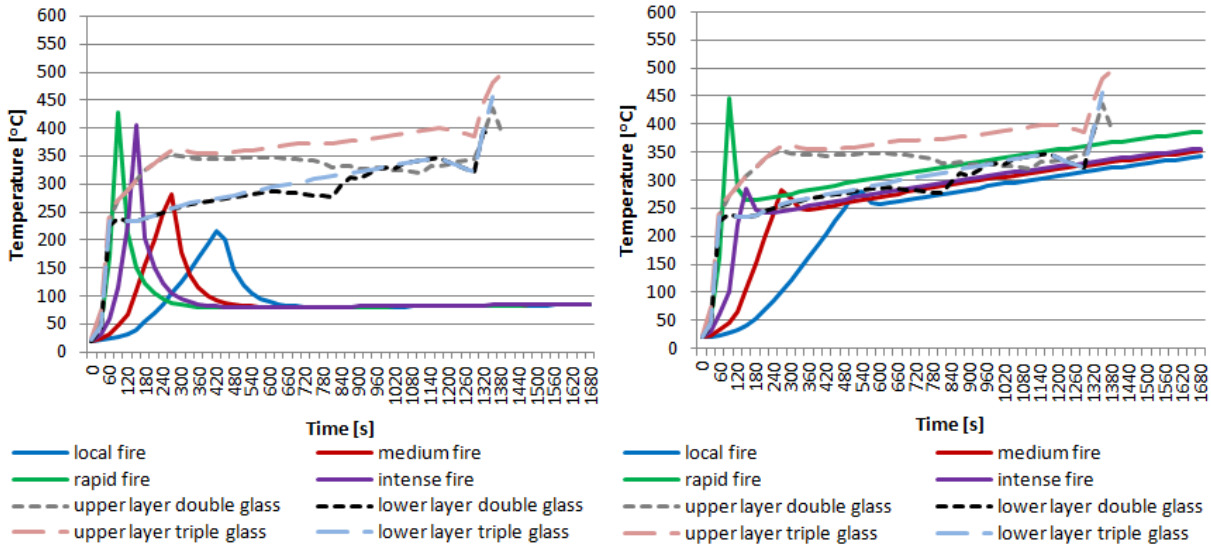

Temperature in the bedroom with a light construction

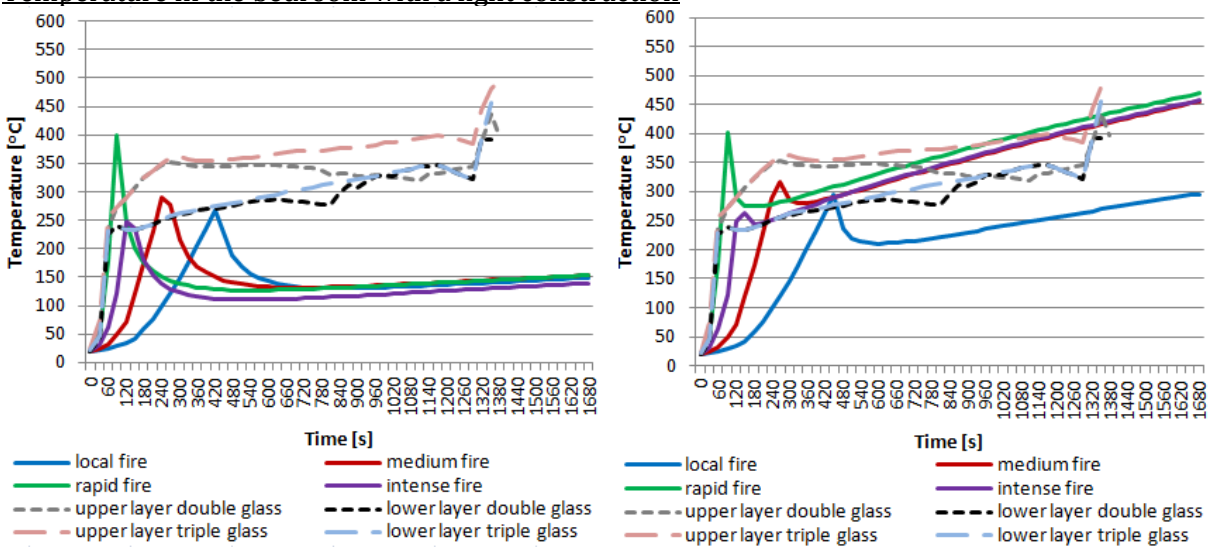

Internal energy in gasvolume

Difference in internal energy in gasvolume in the bedroom with a heavy construction

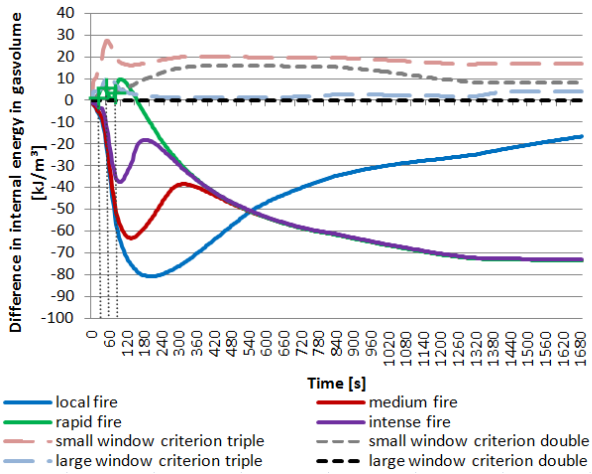

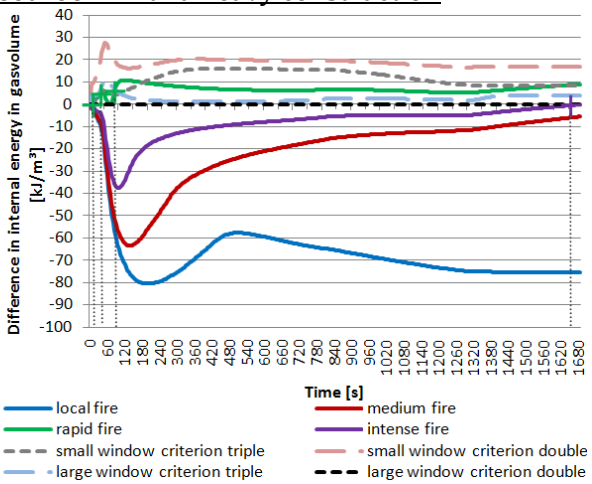

Difference in internal energy in gasvolume in the bedroom with a light construction

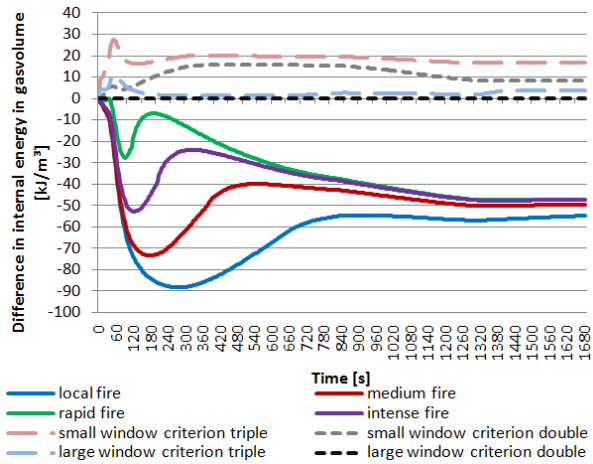

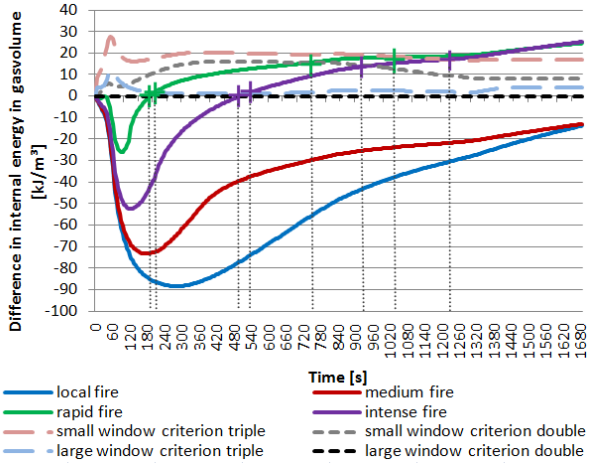

Appendix VII: Input of the simulation model in Voltra

Simulation with stationary material properties

Input materials double glazing					
Layer	Type	λ	ε	ρ	Cp
Timber framing Mohogony	material	0.13	0.90	550	2070
Glass inner pane	material	1.00	0.89	2500	720
Glass outer pane	material	1.00	0.89	2500	720
Timber glazing bead	material	0.13	0.90	550	2070
Kerafix 2000	material	0.06	0.90	96	840
Steal distance spacer	material	50.00	0.90	7800	480

Input cavity's and air layers					
Layer	Type	θ	hc	ρ	Cp
Ambient air	BC_simpl	19.5	-	-	-
Argon cavity	BC_free	-	4.167	1.8	320
Edge cavity	BC_free	-	-	1.1	1000
Air cavity inside spacer	BC_free	-	6.25	1.1	1000

Input Fire					
Simulation	Layer	Type	θa	θr	hc
Large window	Fire curve lower layer	BC_sky	T02	T02	25.0
	Fire curve middle layer	BC_sky	T03	T03	25.0
Small window	Fire curve upper layer	BC_sky	T04	T04	25.0

Simulation with retrieved transient material properties

Input materials double glazing					
Layer	Type	λ	ε	ρ	Cp
Timber framing Mohogony	material	0.13	0.90	550	C03
Glass inner pane	material	L06	0.89	2500	720
Glass outer pane	material	L06	0.89	2500	720
Timber glazing bead	material	0.13	0.90	550	C03
Kerafix 2000	material	L04	0.90	96	840
Steal distance spacer	material	50.00	0.90	7800	480

Input cavity's and air layers					
Layer	Type	θ	hc	ρ	Cp
Ambient air	BC_simpl	19.5	-	-	-
Argon cavity	BC_free	-	4.167	1.8	C01
Edge cavity	BC_free	-	-	1.1	1000
Air cavity inside spacer	BC_free	-	6.25	1.1	1000

Input Fire					
Simulation	Layer	Type	θa	θr	hc
Large window	Fire curve lower layer	BC_sky	T02	T02	25.0
	Fire curve middle layer	BC_sky	T03	T03	25.0
Small window	Fire curve upper layer	BC_sky	T04	T04	25.0

Simulation based on transient material properties and lower ventilation rate

Input Fire					
Simulation	Layer	Type	θa	θr	hc
Large window	Fire curve lower layer	BC_sky	T02	T02	15.0
	Fire curve middle layer	BC_sky	T03	T03	15.0
Small window	Fire curve upper layer	BC_sky	T04	T04	15.0

Simulation based on transient material properties and radiation through refractory bricks

Input Fire					
Simulation	Layer	Type	θa	θr	hc
Large window	Fire curve lower layer	BC_sky	T02	T06	25.0
	Fire curve middle layer	BC_sky	T03	T06	25.0
Small window	Fire curve upper layer	BC_sky	T04	T06	25.0

Simulation based on transient material properties and radiation through refractory bricks and higher ventilation rate

Input Fire					
Simulation	Layer	Type	θa	θr	hc
Large window	Fire curve lower layer	BC_sky	T02	T06	35.0
	Fire curve middle layer	BC_sky	T03	T06	35.0
Small window	Fire curve upper layer	BC_sky	T04	T06	35.0

Defined functions

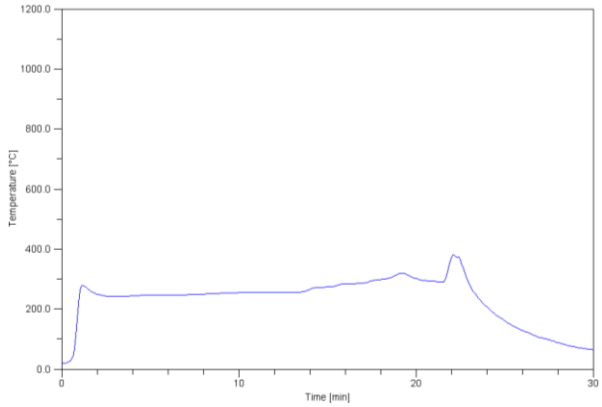

T02: Convective temperature in the fire furnace for the lower layer (measured).

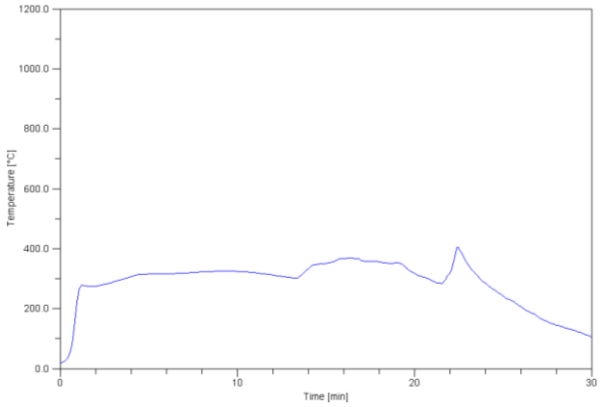

T03: Convective temperature in the fire furnace for the medium layer (measured).

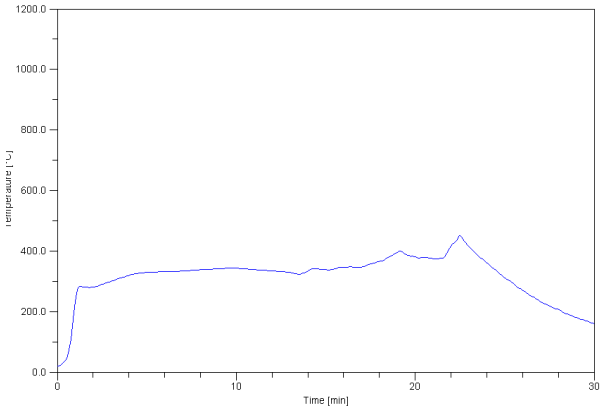

T04: Convective temperature in the fire furnace for the upper layer (measured).

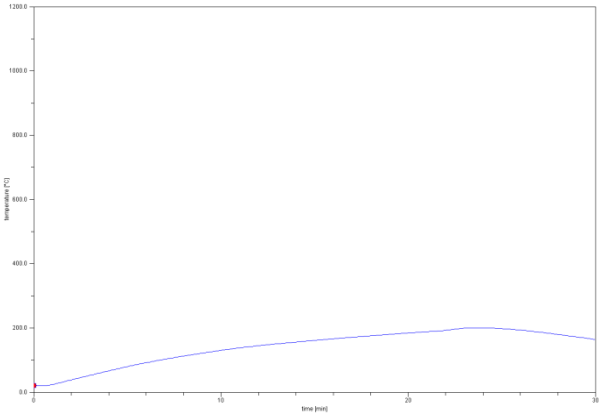

T06: Averaged radiation temperature from the surface temperature of the refractory bricks.

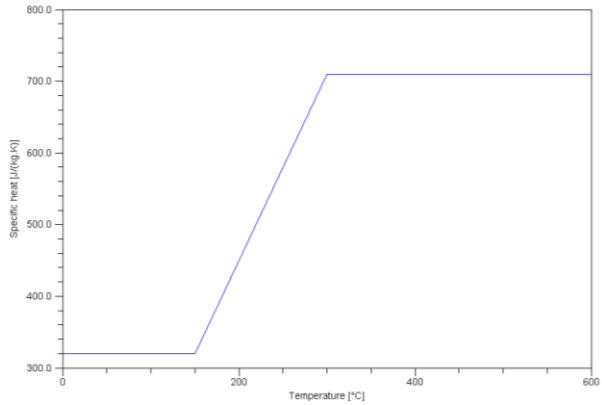

C01: Specific heat of argon cavity.

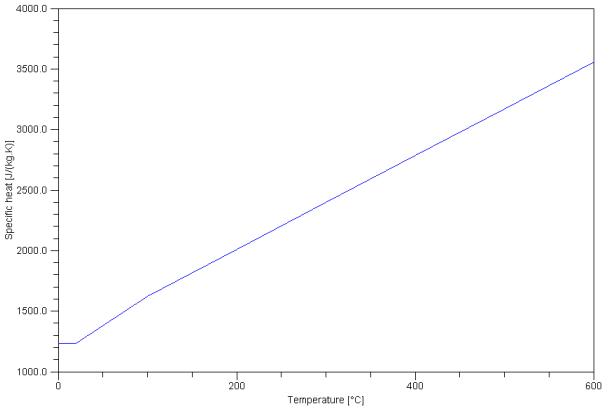

C03: Specific heat Mahogony frame. (www.fs.fed.us).

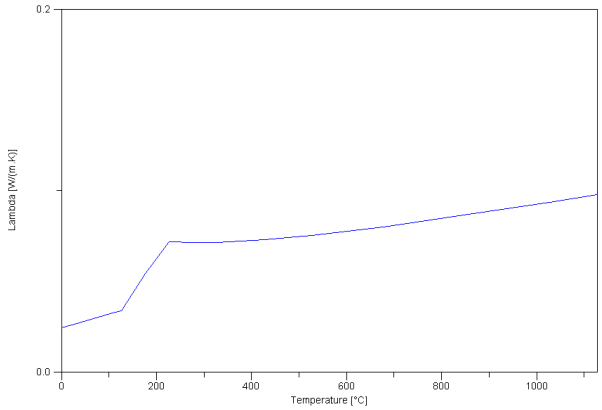

L02: Air cavity.
Kadoya et al (1985)

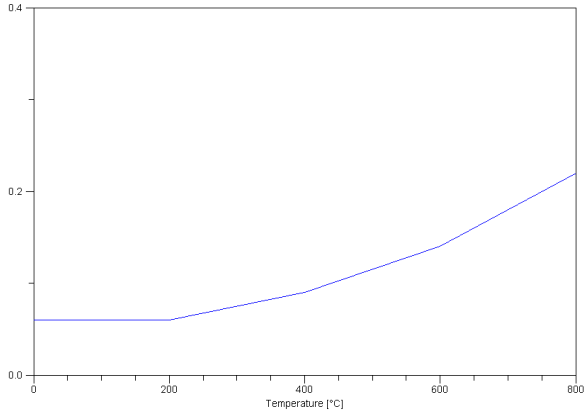

L04: Thermal conductivity Kerafix 2000.
(www.proflex.se)

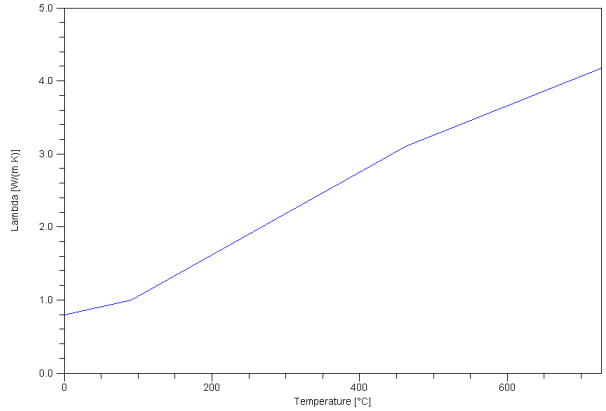

L06: Thermal conductivity SLS glass.
Zeller and Pohl (1971)

Stationary convective heat transfer coefficient for cavity's (www.physibel.be)

convective heat transfer coefficient h_c [W/(m².K)]		temperature difference over the cavity $\Delta\theta$ [°C]									
		0.500	1.000	1.500	2.000	3.000	4.000	5.000	6.000	8.000	10.000
depth of the cavity d [m]	0.001	50.000	50.000	50.000	50.000	50.000	50.000	50.000	50.000	50.000	50.000
	0.002	25.000	25.000	25.000	25.000	25.000	25.000	25.000	25.000	25.000	25.000
	0.003	16.667	16.667	16.667	16.667	16.667	16.667	16.667	16.667	16.667	16.667
	0.004	12.500	12.500	12.500	12.500	12.500	12.500	12.500	12.500	12.500	12.500
	0.005	10.000	10.000	10.000	10.000	10.000	10.000	10.000	10.000	10.000	10.000
	0.006	8.333	8.333	8.333	8.333	8.333	8.333	8.333	8.333	8.333	8.333
	0.007	7.143	7.143	7.143	7.143	7.143	7.143	7.143	7.143	7.143	7.143
	0.008	6.250	6.250	6.250	6.250	6.250	6.250	6.250	6.250	6.250	6.250
	0.009	5.556	5.556	5.556	5.556	5.556	5.556	5.556	5.556	5.556	5.556
	0.010	5.000	5.000	5.000	5.000	5.000	5.000	5.000	5.000	5.000	5.000
	0.011	4.545	4.545	4.545	4.545	4.545	4.545	4.545	4.545	4.545	4.545
	0.012	4.167	4.167	4.167	4.167	4.167	4.167	4.167	4.167	4.167	4.167
	0.013	3.846	3.846	3.846	3.846	3.846	3.846	3.846	3.846	3.846	3.846
	0.014	3.571	3.571	3.571	3.571	3.571	3.571	3.571	3.571	3.571	3.571
	0.015	3.333	3.333	3.333	3.333	3.333	3.333	3.333	3.333	3.333	3.333
	0.016	3.125	3.125	3.125	3.125	3.125	3.125	3.125	3.125	3.125	3.145
	0.017	2.941	2.941	2.941	2.941	2.941	2.941	2.941	2.941	2.941	3.145
	0.018	2.778	2.778	2.778	2.778	2.778	2.778	2.778	2.778	2.920	3.145
	0.019	2.632	2.632	2.632	2.632	2.632	2.632	2.632	2.653	2.920	3.145
	0.020	2.500	2.500	2.500	2.500	2.500	2.500	2.500	2.653	2.920	3.145
	0.025	2.000	2.000	2.000	2.000	2.106	2.318	2.497	2.653	2.920	3.145
	0.030	1.667	1.667	1.671	1.839	2.106	2.318	2.497	2.653	2.920	3.145
	0.035	1.429	1.460	1.671	1.839	2.106	2.318	2.497	2.653	2.920	3.145
	0.040	1.250	1.460	1.671	1.839	2.106	2.318	2.497	2.653	2.920	3.145
	0.045	1.159	1.460	1.671	1.839	2.106	2.318	2.497	2.653	2.920	3.145
	0.050	1.159	1.460	1.671	1.839	2.106	2.318	2.497	2.653	2.920	3.145
	0.060	1.159	1.460	1.671	1.839	2.106	2.318	2.497	2.653	2.920	3.145
	0.070	1.159	1.460	1.671	1.839	2.106	2.318	2.497	2.653	2.920	3.145
	0.080	1.159	1.460	1.671	1.839	2.106	2.318	2.497	2.653	2.920	3.145
	0.090	1.159	1.460	1.671	1.839	2.106	2.318	2.497	2.653	2.920	3.145
	0.100	1.159	1.460	1.671	1.839	2.106	2.318	2.497	2.653	2.920	3.145

Stationary convective heat transfer coefficient for exterior environments (www.physibel.be)

convective heat transfer coefficient h_c [W/(m².K)]		temperature difference object -environment $\Delta\theta$ [°C]			
		5	10	20	40
air velocity v [m/s]	0.5	7	8	9	11
	1	9	10	11	13
	2	12	13	15	16
	3	19	20	21	23
	4	25	26	27	28
	5	30	31	32	34

Appendix VIII: Calibration of the simulation model

Large window

Stationairy material propeties

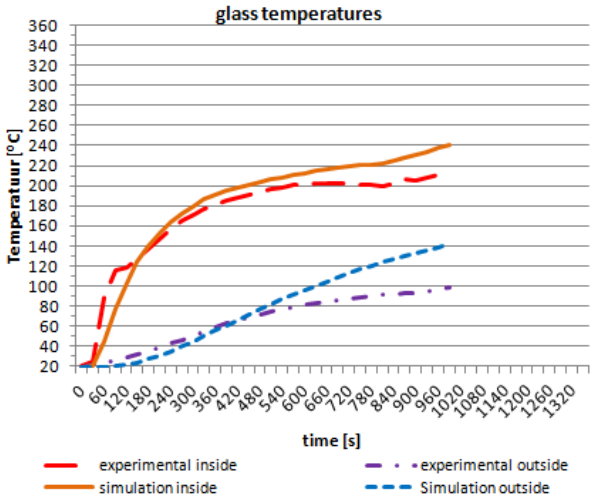

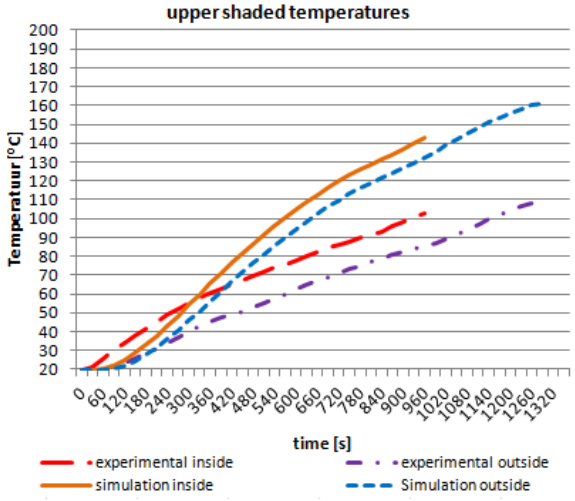

Transient material properties

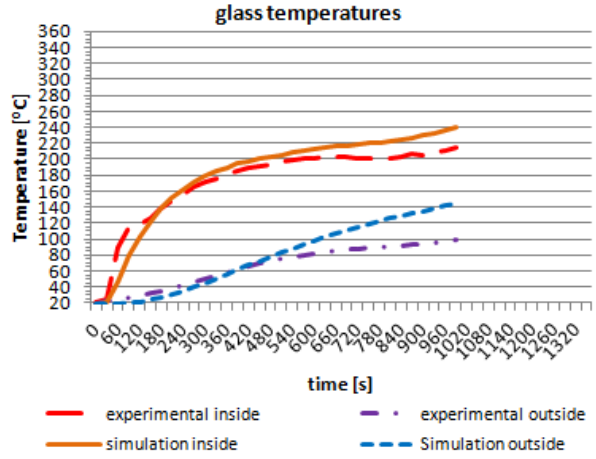

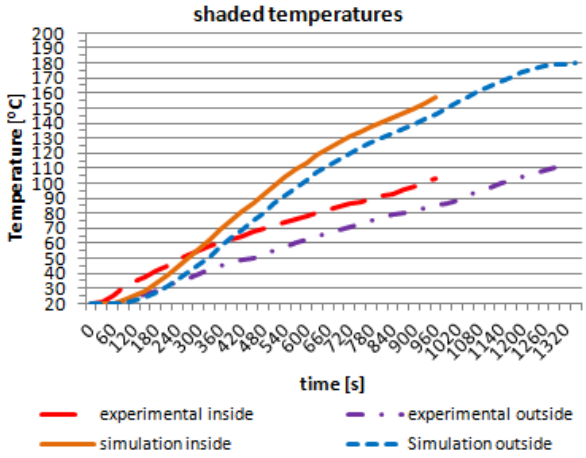

Transient material properties, radiation derived from refractory bricks

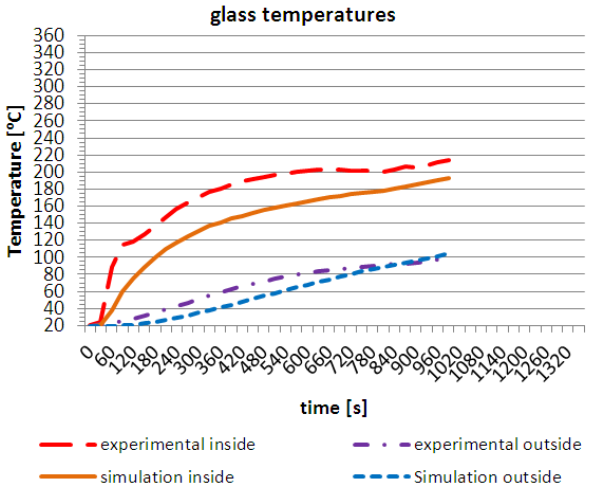

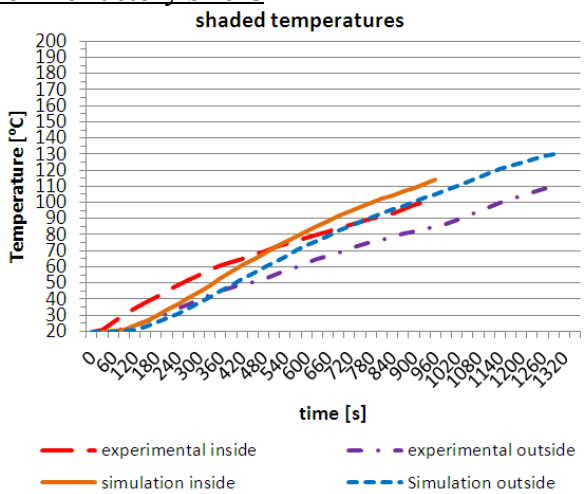

Transient material properties, radiation derived from refractory bricks with higher h_c 35

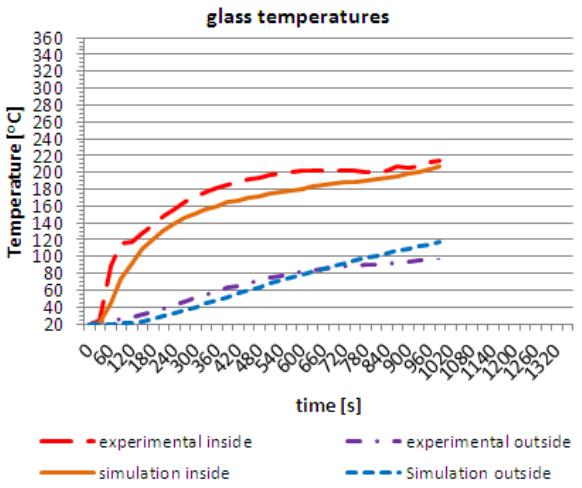

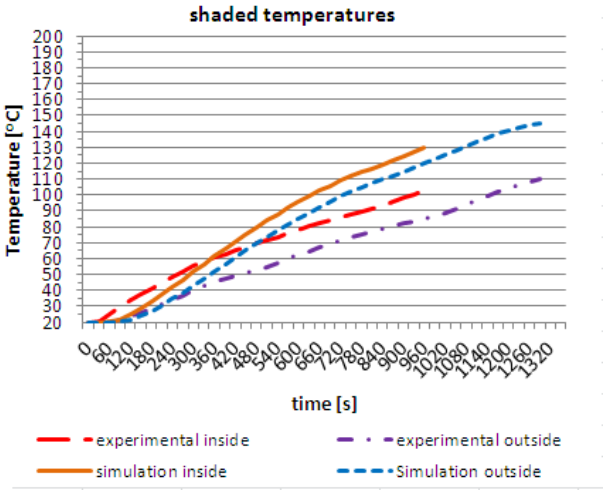

Transient material properties with adjusted h_c to 15

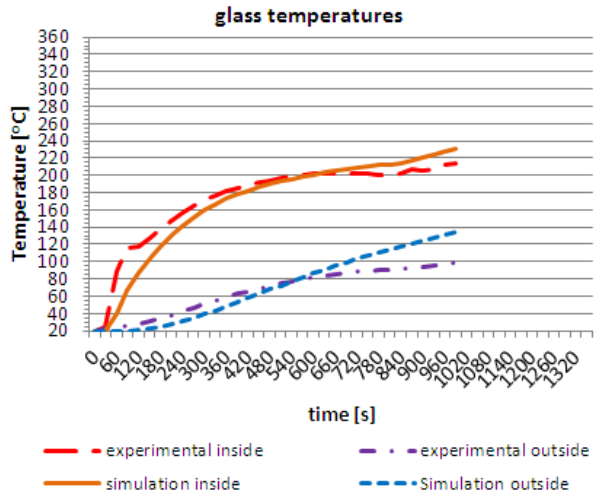

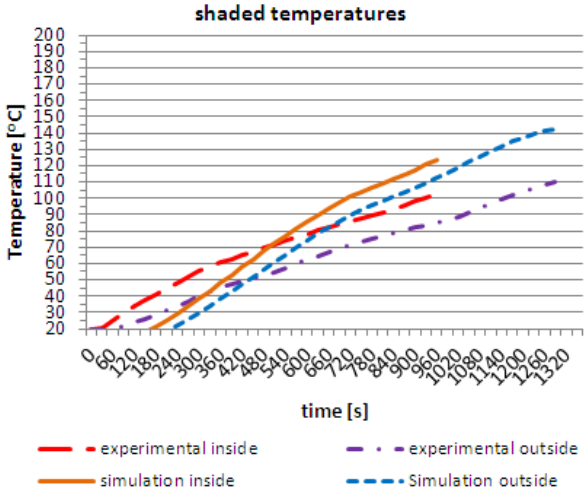

Small window

Stationairy material propeties

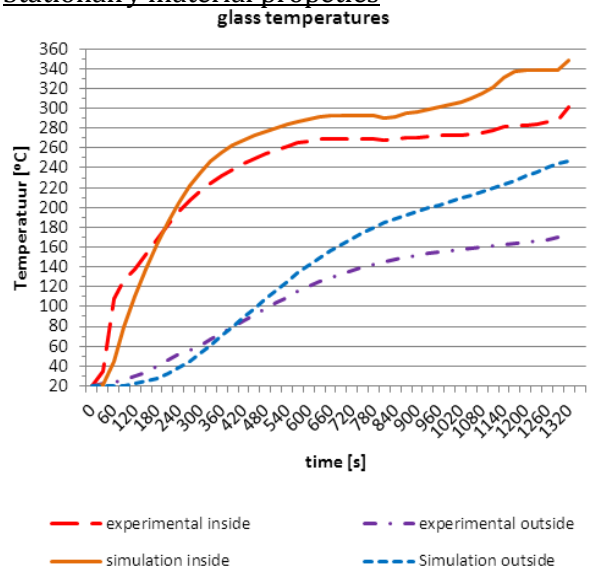

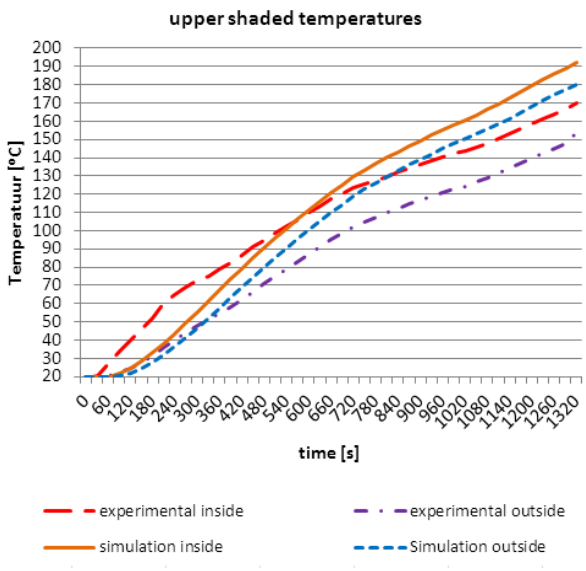

Transient material properties

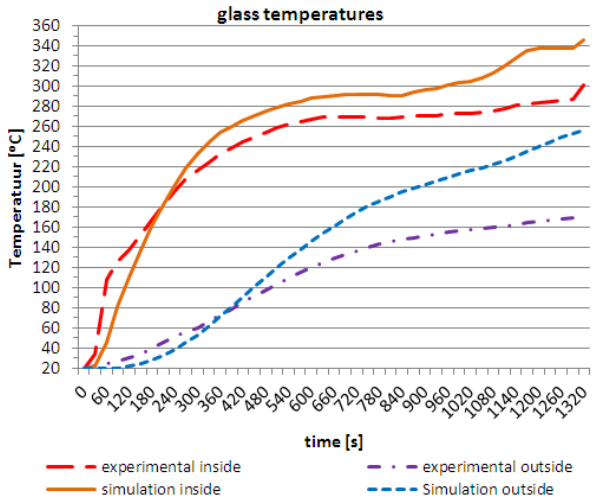

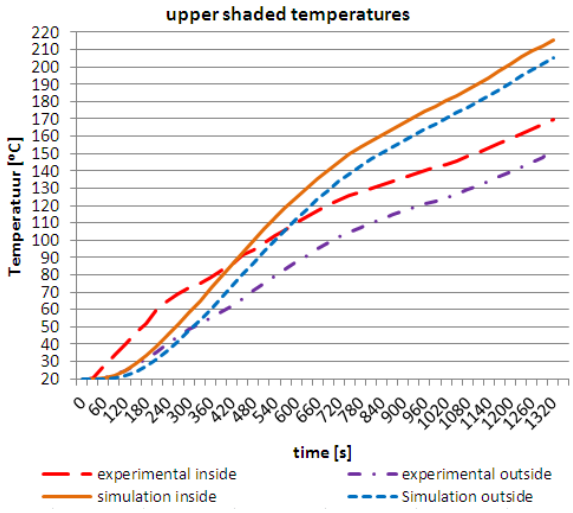

Transient material properties with adjusted h_c to 15

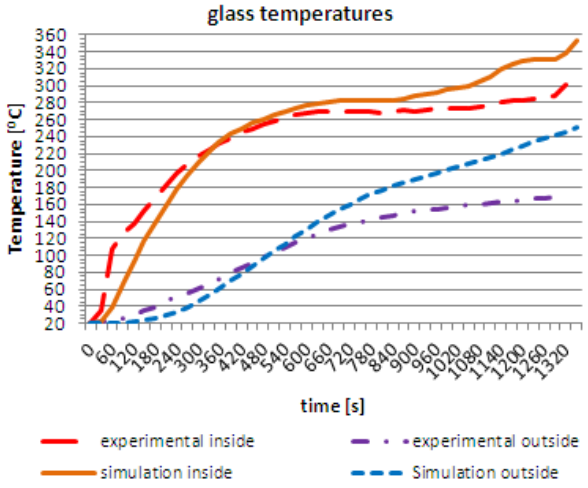

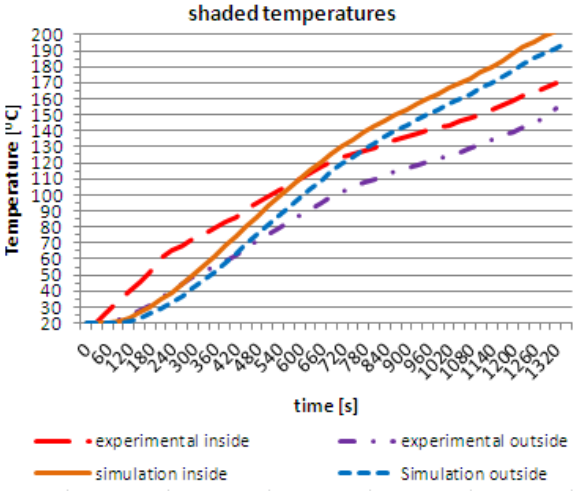

Transient material properties, radiation derived from refractory bricks

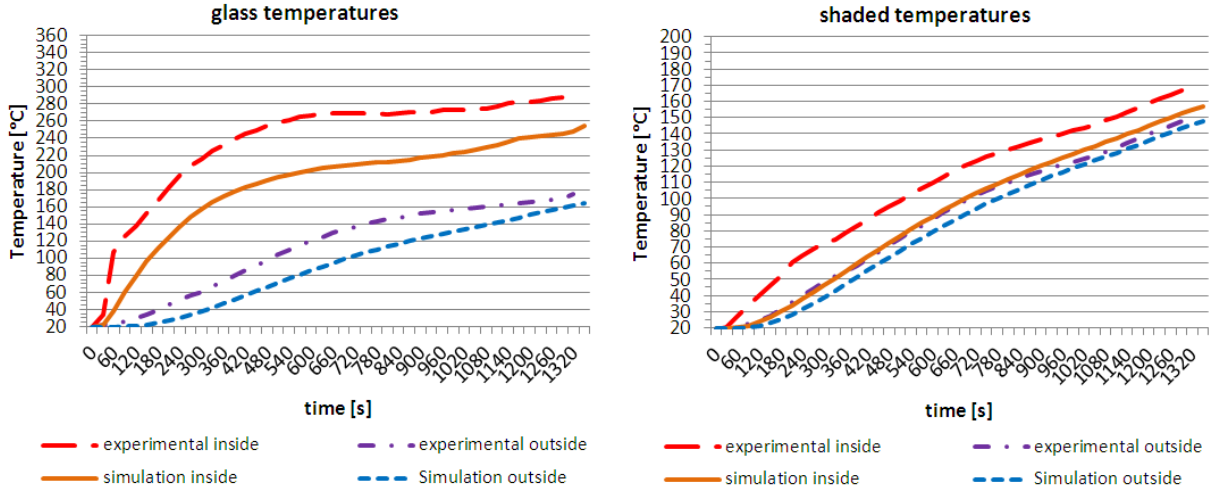

Transient material properties, radiation derived from refractory bricks with h_c 35